A Finite Element Model of the Current Distribution in the Skin

Master Thesis

10th semester

Project group: 1085b

Mathilde Pedersen

Department of Health Science and Technology
Aalborg University 2009

The Faculty of Engineering, Science and Medicine
Aalborg University

Title:
A Finite Element Model of the Current distribution in the skin

Project period:
10th semester
February 1st 2009 -
June 1st 2009

Project group:
1085b

Group members:
Mathilde Pedersen

Supervisor:
Carsten Dahl Mørch
Ole Kæseler Andersen

Number of copies: 4

Number of pages: 63

In relation to many different applications it is desired to preferentially activate cutaneous nociceptors and avoid activating other sensory organs and nerve fibers. To enable this, it is essential that the intensity of the current density in upper most layers of the skin, are larger than in the rest of the skin, due to the locations of the nociceptors.

A finite element model of the electric properties of the skin was developed to examine the distribution of the current density in the skin when a concentric surface electrode was utilised. The diameter of the inner cathode could be changed and it was examined whether a small cathode more preferentially than a larger cathode would stimulate nociceptors.

The current density in the upper layers, at the edge of the cathode was larger compared to the rest of the skin when a small cathode was utilised than when a large cathode was utilised. It could, therefore, be concluded that small electrodes, more preferentially will stimulate nociceptors than a large electrode.

The model consisted of two layers; stratum corneum and the cellular epidermis combined with dermis. The model did not included any skin appendages. The intensity of the current density was examined, to determine whether the nociceptors were activated. A model of the nerve fibers should be included in future models.

Preface

This report describes the work performed by Mathilde Pedersen as the 10th semester master thesis, at the Department of Health Science and Technology, Aalborg University, Denmark.

The study is written under the area of specialisation of Medical Systems in the period from February 1st - June 4th 2009.

The author would like to thank Mathijs Kurstjens for providing assistance in the laboratory.

Aalborg University, June 2009

Mathilde Pedersen

Contents

I Preface 1

1 Introduction 3
1.1 Studies regarding nociceptive stimulation . . . 4

2 Thesis Statement 9
2.1 Electrode Design . . . 9
2.2 Solution Model . . . 10

II Preliminary Analysis 13

3 The layers of the skin 15
3.1 Skin physiolology . . . 15
3.2 Thickness of layers of the skin . . . 19

4 The electric properties of the skin 23
4.1 Electric Fields . . . 23
4.2 Conducting and dielectric materials . . . 25
4.3 Frequency dependence of the electric properties of the skin . . . 29
4.4 Literature study regarding the electrical properties of the skin . . . 31

III Solution 37

5 Finite Element Modeling 39
5.1 Selection of law of physics . . . 39
5.2 Drawing of the geometry . . . 41
5.3 Setting of material properties, boundary conditions and initial conditions . . . 42
5.4 Meshing . . . 43

6 Validation 45

7 Results 47

IV Synthesis 57

8 Discussion 59
8.1 Methodology . . . 59
8.2 Pathways of the Current flow . . . 60

9 Conclusion **61**

Bibliography **63**

A Verification of the model **65**

Preface

I

1 Introduction

This project examines electric currents applied to the skin in order to evoke a pain experience. Current is applied to the body through the skin in many different applications. The pain-related applications are among others; itch relief [Nilsson, Levinsson & Schouenborg 1996], [Yosipovitch, Carstens & McGlone 2007], recordings of pain-related evoked potentials in order to evaluate cranial and somatic nociceptive systems [Inui, Tran, Hashoyama & Kakigi 2001], [Katsarava, Ayzenberg, Sack, Limmroth, Diener & Kaube 2006], long-lasting modification of synaptic transmission in order to understand the cellular mechanisms underlying learning and memory function [Jung, Rottmann & Ellrich 2009], [Klein, Magerl, Hopf, Sandkuhler & Treede 2004]. Itching is, however, not defined as the same experience as a pain and might have its own separate set of C-fibers only signaling information concerning itch [Nilsson et al. 1996], [Yosipovitch et al. 2007].

All the applications listed above faces the same problem regarding costimulation of different types of nerve fibers, when electric stimulation is used. Nociceptors only responds when substantial stimuli are applied as a sign of danger. Thus, the nociceptors have a higher threshold than other cutaneous sensory receptors. This means that the other sensory receptors are more easily activated than the nociceptors [Schibye & Klausen 2004]. However, it might not even be the receptors which are stimulated when current is applied, but the nerve fibers, attached to the receptors. These might be activated directly, if the current exceeds their threshold. It is therefore not straightforward to stimulate the nociceptors without also stimulating the other receptors.

The axons from the nociceptors that provide information regarding the location and intensity of noxious stimuli to the central nervous system are C, Aδ, and Aβ fibers [Djouhri & Lawson 2004], [Andersen 2007], [Kandel, Schwartz & Jessell 1991]. It is debated whether the Aβ fibers relay information about the noxious stimuli to the central nervous system, however, recent studies have shown that the Aβ is included in the information processing in the central nervous system [Djouhri & Lawson 2004]. It is, however, often desired to avoid stimulating the Aβ since they primary convey information regarding mechanoreception and not exclusively nociception [McMahon & Kolzenburg 2006]. Thus, in most applications it is only desired to activate the nociceptive C or Aδ fibers and not the Aβ fibers.

The conduction velocity of the nerve fibers is often used to validate whether the desired fibers have been activated. The C fibers are thin and unmyelinated and have conduction velocities less than 2.5 m/s. The A fibers are myelinated and does therefore conduct the signal faster than the C fibers. Aδ fibers have a conduction velocity between 4-30 m/s while the Aβ fibers have conduction velocities between 30-65 m/s [Andersen 2007], [Kandel et al. 1991]. Another more subjective method indicating which nerve fibers are activated can also be utilised. A burning sensation is felt and a flare reaction is developed in the vicinity of the stimulating electrode when the C fibers are activated. A pricking pain is felt when the Aδ fibers are stimulated [Martini 2004]. It must be stressed that this is a subjective observation and it cannot solely be used to validate that the aimed nerve fibers have been activated.

The nociceptors are free nerve endings reaching into the lower layer of the epidermis, whereas other cutaneous sensory organs lie in the dermis [Kahle & Frotscher 2003], [Schibye & Klausen 2004]. Figure 1.1 shows the position of some cutaneous sensory organs.

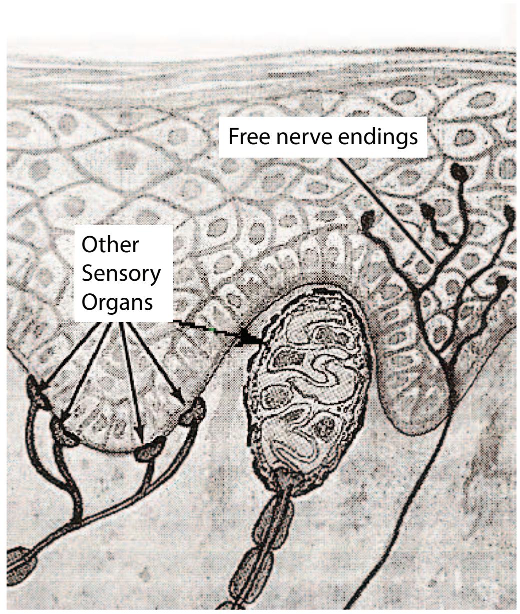

Figure 1.1: shows the position of the free nerve endings in relation to other sensory organs [Schibye & Klausen 2004]

In order to preferentially stimulate the nociceptors and not the other sensory receptors or nerve fibers it is requisite that the intensity of the stimulating current is highest in the superficial layers of the skin. It is difficult to obtain sufficient nociceptive input by utilising conventional transcutaneous nerve stimulation with large surface electrodes, since it causes an activation of Aβ fibers at much lower current strengths than nociceptive Aδ and C fibers.

1.1 Studies regarding nociceptive stimulation

Several groups have examined the selective stimulation of the nociceptive fibers by means of the current flow. Four articles are shortly reviewed in the following. The first two attempted to stimulate the nociceptive fibers by utilising small needle electrodes, whereas the two latter utilised concentric surface electrodes.

Nilsson et al. [1996] developed a new technique termed cutaneous field stimulation (CFS) to relieve itch. Itch is a major symptom in many systemic and skin diseases and can cause considerable suffering for the patient. Itch is instantly relieved when the skin is scratched mechanically, but due to skin injury the itch often increases over time. Very little is known about the neural mechanisms underlying itch and itch control. The mechanisms underlying itch may be dependent on the activation of nociceptors. It has been suggested that there is a separate set of C-fibers that only signal information concerning itch [Yosipovitch et al. 2007]. This assumption indicates that the nociceptive input somehow masks the activity in the itch pathways or alternatively that the mechano-nociceptive input may actively inhibit central itch pathways.

CFS was compared to transcutaneous electrical nerve stimulation (TENS). TENS is known to inhibit itch, but not sufficiently for practical clinical purposes. The aim of the study conducted by Nilsson et al. [1996] was to examine whether CFS more efficiently than TENS relives itch.

CFS utilizes a flexible rubber plate with sixteen needle-like electrodes fixed with regular distances of 2 cm intervals. The needle-like electrodes were meant to protrude stratum corneum, when the electrode plate was pressed gently toward the skin and the electrode tips were thought to be placed adjacent to the receptors in the epidermis and the superficial parts of the dermis. This was, however, not proved. The CFS caused no visual damage to the skin. By utilising small needle electrodes it was expected that the current density was high close to the receptors in the epidermis and the superficial parts of the dermis and thereafter would decrease rapidly. In such case the receptors close to the tip of would preferentially be activated and the receptors and nerve fibers further away would not to the same extent be influenced. A surface electrode was used for the TENS. Limited information was stated regarding the TENS method.

The intensity of the stimulation was increased to perception threshold and thereafter to twice the intensity of the perception threshold where it was maintained the rest of the stimulation time. This procedure was conducted for both CFS and TENS. The total stimulation time was 25 minutes. CFS and TENS were applied to the right arm prior to the induced itch. The itch was induced either immediately after or two hours after the CFS or TENS were applied. The itch was induced by transdermal iontophoresis of histamine. The itch was induced on both the ipsilateral and the contralateral arm. The measurements of the intensity of the itching were done in one hour.

A pin-prick with a burning character and a slight buzzing sensation were felt during CFS. In addition a flare reaction always developed around each electrode in the CFS plate indicating an axon reflex in nociceptive C-fibers. The CFS still produced a burning sensation indicating an activation of the nociceptive C-fibers, during a selective pressure block of the superficial radial nerve, which causes a block of the propagation of the A fibers.

The peaking of itch sensation occurred after 0.5 to 10 minutes after discontinuing the imposed histamine. In the next 40 - 60 minutes the itching gradually decreased. The results of the comparison between the effects of CFS and TENS are shown on figure 1.2.

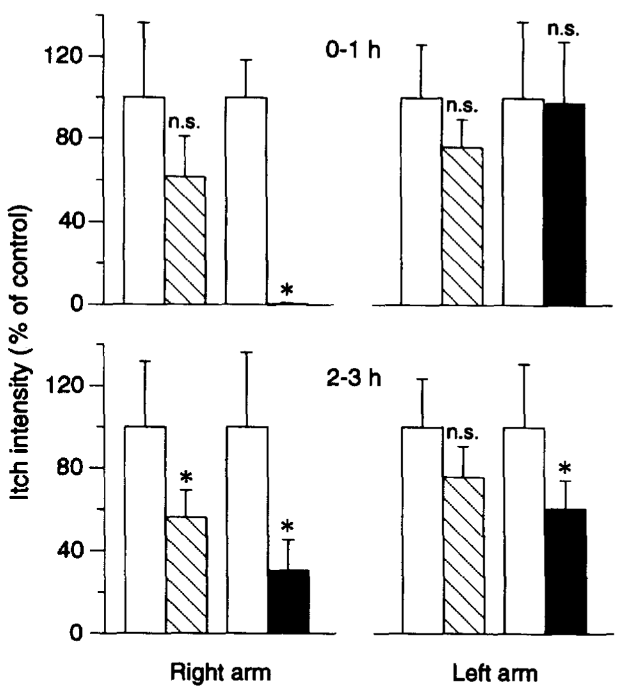

Figure 1.2: shows the results obtained by Nilsson et al. [1996]. The figure shows the itch intensity in percent of the controls. The time of the application and measurement of the itch is given in the middle; the upper figure is the measurements 0-1 hour and the lower is after 2-3 hours after stimulation. The unfilled bars indicate the controls, the hatched show the results from the TENS and the black show the results from CFS. Significant difference is indicated with an asterisk.

CFS significantly abolished itch within the conditioned skin area during the first hour after the histamine was applied. However there was no significant effect on the contralateral side. A reduction in the intensity of the itching was found for TENS, this was however not significant. In the case where the itching was applied two hours after the CFS or

TENS a significant reduction in the ipsilateral arm for both stimulation types were found. In the contralateral arm only a significant reduction in the itching for the CFS compared with the control group were found.

The results obtained by Nilsson et al. [1996] showed improved inhibition of the itching compared with a control group when CFS was utilised instead of TENS. TENS did probably not inhibit the itch as effectively since it preferentially activated the large myelinated fibers and not as effectively as the CFS affected the nociceptors or the separate set of itch mediating C-fibers.

Inui et al. [2001] recorded evoked potentials induced by three different types of stimulation; conventional transcutaneous electrical stimulation, laser stimulation and epidermal electrical stimulation. The objective of the article was to investigate the brain responses evoked by the pain-related epidermal stimulation in comparison with those evoked by more conventional methods. The brain responses were investigated by measuring the somatosensory evoked potentials.

It is possible to evoke pain related responses by stimulating the Aδ and C fibers with a CO_2 laser. The laser does however have some technical difficulties in practical use, since it in order to cause an effective pain, might cause heat burns of the skin. The conventional electrical stimulation does not cause any damage to the skin but does not selectively stimulate the nociceptive Aδ and C fibers. It will as earlier mentioned also stimulate the myelinated fibers with large diameter, which has a lower threshold than the nociceptive fibers. The third method utilised was epidermal electrical stimulation, which was a modification of the method used by Nilsson et al. [1996]. This method utilised a specially made single electrode. The electrode used a push-pin-like needle electrode, which was developed especially to stimulate the Aδ fibers in a very small area. The length of the needle was 0.2 mm and had a stop device preventing from being pressed further into the skin. The electrode is shown on figure 1.3.

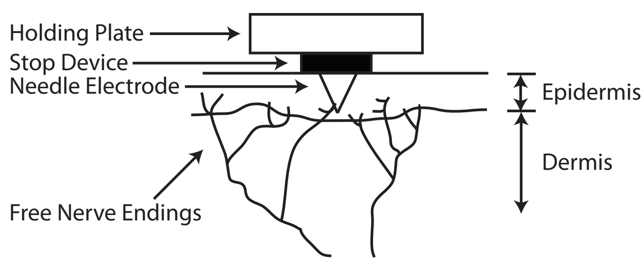

Figure 1.3: shows the needle electrode utilised by Inui et al. [2001]. The figure is not to scale; the intracutaneous area is enlarged.

As in the study conducted by Nilsson et al. [1996] the small needle electrode was thought to protrude stratum corneum when the electrode plate is pressed gently against the skin. The electrode tip of the needle electrode is, thereby, expected to be inserted against the nerve endings of the thin myelinated fibers. It must, however, be stressed that this only is an assumption and not assumption correct, since the thickness of stratum corneum varies between body sites and individuals [Sandby-Møller, Poulsen & Wulf 2003], [Martini 2004], [Standring 2005].

The intensity was adjusted to each subject and was at a level where it produced a definite pain sensation. The level was determined prior to the experiment. The needle electrode did not cause any bleeding or visible damage to the skin. There were no observation of flare reactions, which is an indication of activation of C fibers, this is probably due to a higher electrical threshold of C fibers than of Aδ fibers.

Electroencephalography was recorded after each stimulus condition and the conduction velocity was calculated. The conduction velocities found for the epidermal electrical stimulation was in agreement with the conduction velocities found when the laser was utilised. The laser is known to stimulate the Aδ fibers and can, therefore, be used for the validation. In addition the stimulation with the epidermal electrical stimulation produced a well-defined pricking pain without definite tactile sensations as seen when Aδ fibers are stimulated. The conduction velocity found when conventional transcutaneous electrical stimulation was utilised corresponded to the conduction velocity of Aβ fibers.

The overall conclusion of the article was that epidermal electrical stimulation more effectively stimulated nociceptive fibers than the conventional transcutaneous electrical stimulation did. It could, however, not be determined whether the epidermal electrical stimulation also activated the A fibers, due to their low electric threshold.
Katsarava et al. [2006] proposed a novel technique of noninvasive transcutaneous stimulation the peripheral nociceptive fibers to avoid using an invasive electrode. A concentric surface electrode was therefore utilised instead of using small needles as Nilsson et al. [1996] and Inui et al. [2001]. The electrode had a small anode-cathode distance and produced a high current density at low current intensities. The configuration of the electrode was ought to limit the depolarisation to the superficial layers of the dermis, which contains the nociceptive Aδ fibers. To the left in figure 1.4 the expected electric fields produced by the new concentric electrode are shown and to the right the expected electric fields of a conventional electrode are shown.

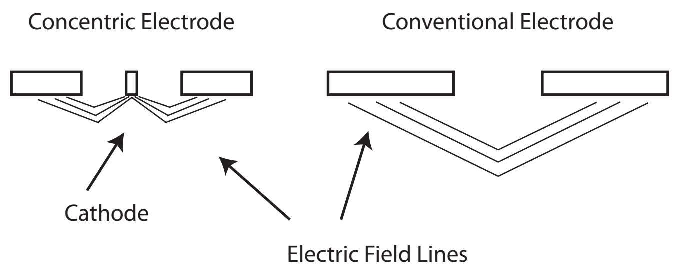

Figure 1.4: illustrates, to the left, the expected electric field generated by the new concentric electrode and to the right the expected electric field of a conventional electrode is shown. The figure is not to scale. Redrawn from [Katsarava et al. 2006]

The central metal cathode of the concentric electrode had a diameter of 0.5 mm. between the cathode and the anode isolation were inserted which had an external diameter of 5 mm. The outer anode ring had an external diameter of 6 mm.

In the study conducted by Katsarava et al. [2006] recordings of pain-related evoked potentials were elicited by the concentric electrode. As a part of the study, the mean conduction velocity was used to demonstrate that the Aδ fibers and not the Aβ fibers were activated. Individual perception and pain thresholds were determined for the participating subjects. The stimulation intensity when the experiment was conducted was set to 1.5 of the individual pain threshold.

The found mean conduction velocities were between 11.6 $\pm$ 5.1 m/s. This falls in the range of the conduction velocity of Aδ fibers. In addition a pinprick-like pain which is characteristic for pain elicited by Aδ fibers occurred during the stimulation. This implies that the Aδ fibers were stimulated when the concentric surface electrode was utilised.

In studies regarding long-term potentiation and depression different electrode designs have been utilised in order to preferentially activate nociceptors. Long-term potentiation and depression are used to obtain a long-lasting modification of the synaptic strength [Klein et al. 2004], [Jung et al. 2009]. It is an intensively studied cellular model of learning and memory formation. Klein et al. [2004] and Jung et al. [2009] did not perform studies comparing different electrodes but utilised specially designed electrodes in order to optimise the selective activation of nociceptors.

Klein et al. [2004] applied electrical stimuli through punctate electrodes with a diameter on 200 μm. Ten of these electrodes were mounted in a small circular plastic frame placed on the surface of the skin. All ten electrodes were stimulated simultaneously. Single pulses at detection threshold intensity were perceived as painful indicating that superficial nociceptors preferentially were activated. To examine whether the nociceptors were activated the increase in cutaneous blood flow were monitored by Laser Doppler imaging. An increase of skin perfusion also known as flare was observed.

Jung et al. [2009] aimed to optimise the stimulation parameters for long-term depression on nociception and pain and examined the effect of stimulation frequency, number of electric pulses, intensity and repetition. The utilised electrode was designed as the one used by Katsarava et al. [2006]. The dimensions of the electrode were, however, different; the small central cathode had a diameter on 1 mm and the larger ring anode had an inner diameter on 8 mm and an outer diameter on 24 mm. A well localized sharp sensation was felt during stimulation with the concentric surface electrode. Thus, it is presumed that Aδ fibers are activated. No further insurance of Aδ activation was reported by Jung et al. [2009].

From the above reviewed articles it becomes evident that the applicability of preferentially stimulation of the nociceptors is manifold. In addition, many different approaches have been tried in order to increase the activation of the nociceptors and avert stimulation of the non-nociceptive nerve fibers.

The small needle electrodes used by Nilsson et al. [1996] and Inui et al. [2001] are controversy since it is claimed they are non-invasive but still penetrate the skin. According to the articles the electrodes did not cause any visible damage to the skin. Hence, it is not known whether the electrodes actually penetrate the skin or whether the skin merely is compressed. Even if the electrodes are thought to penetrate the skin, the small needle electrodes are not versatile, due to differences in the thickness of the skin between body sites and among individuals. The thickness of the skin must, therefore, be found for each stimulation site and the needle adjusted to fit the individual site. It must therefore be stressed that it is unknown whether the tip of the needle electrode, as illustrated in figure 1.3 is placed adjacent to the free nerve endings of the nociceptors.

It is, however, not known whether the design of the concentric surface electrodes utilised by Katsarava et al. [2006] and Jung et al. [2009] could be optimised. The electric field lines shown on figure 1.4 are only illustrations and the flow of the resulting current can only be conjectural.

Thesis Statement

2

The introduction presented different attempts to preferentially activate nociceptors. This included both small needle electrodes and concentric surface electrodes.

The versatility of the small needle electrodes are questioned due to differences in the thickness of the skin between body sites and among individuals. It is, therefore, not ensured that the tip of the needle electrode actually is placed adjacent to the nociceptors. Instead the concentric surface electrode can be utilised. It is not, to the same extent as the small needle electrodes, dependent on the location of the nociceptors. The activation of nociceptors with a concentric surface electrode is, however, more dependent on the dimensions of the electrode. In order to optimise the concentric surface electrode, the effect of the electrode size must be clarified and the following hypothesis is, therefore, stated:

A concentric surface electrode with a small diameter will cause the applied current to flow in the more superficial layers of the skin, than a concentric surface electrode with a larger diameter.

To test the hypothesis it is essential to be able to know how the resulting current flows in the skin. It is, however, not possible to monitor the current flow in vivo. Instead a model of the electric properties of the skin must be developed. In the following sections the electrode design and the solution model are presented.

2.1 Electrode Design

The concentric surface electrode used to test the hypothesis consists of two parts; an inner electrode functioning as cathode and an outer electrode functioning as anode. The electrode is illustrated on figure 2.1.

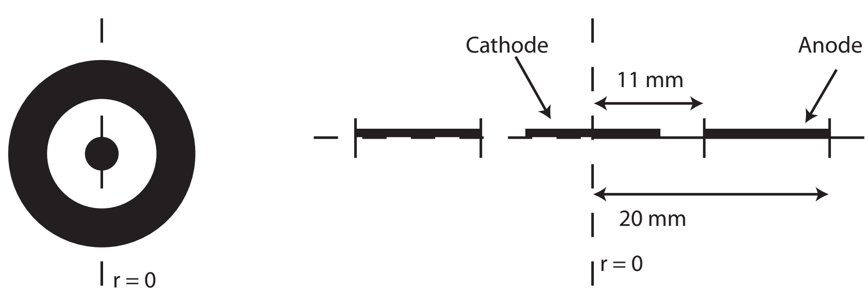

Figure 2.1: illustrates the concentric surface electrode utilised to test the hypothesis. To the left it is seen from the above and to the right from the side

The anode and the cathode consist of stainless stell. The size of the anode is fixed; the inner diameter is 22 mm and the outer diameter is 44 mm. The diameter of the cathode can, however, be changed between the following diameters; 0.9 mm, 4 mm, 8 mm, 12 mm and 20 mm. The space between the anode and the cathode is isolated. A picture of the concentric electrode is shown in figure 2.2.

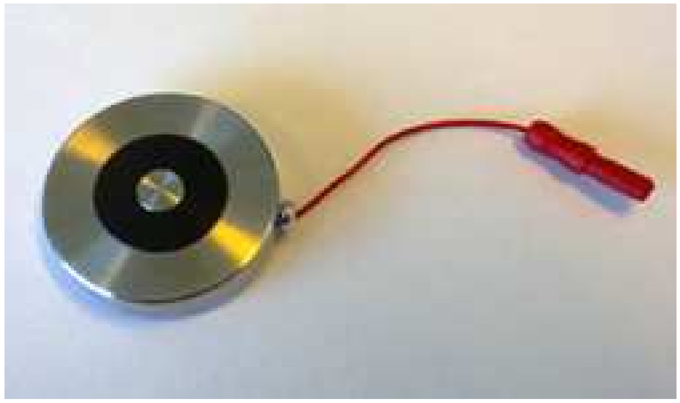

Figure 2.2: shows the concentric surface electrode utilised to test the hypothesis. The outer electrode is the the anode and the inner the cathode.

2.2 Solution Model

To test the hypothesis stated previously it must be known how the current flows in the skin. This is, however, not possible to monitor the paths of the current flow in vivo. Instead a model of the electric properties of the skin can be utilised to monitor the applied current and, thus, test the hypothesis.

Many different approaches can be utilised in order to develop a model of the electric properties of the skin, e.g., an electric analogy can be utilised, this implies that the electric properties of the skin are modeled as electric components. Likewise, it is possible to develop a model of the skin by means of finite element modeling. In addition to the electric properties of the skin, it is possible to include the physical dimensions of the skin, when applying a finite element model.

It is chosen to make a model which is more descriptive, than explanatory. I.e., the model will primarily reflects the phenomenas characterising the electric properties in skin. The applied theories are not in any great extent connected to the microanatomy of the skin, but enable the development of a model which is an electrical equivalent of the skin.

The model which is developed devides the skin into layers according to their electric properties. Thus, it focuses on the components of the skin, which make the larges contribution to the electric properties. Hence, the physiology of the skin must be known prior to the development of the model in order to devide the skin into layers. Hereafter, the electric properties of the different layers can be determined. This is done by a litterature survey. The steps accomplished in the development of the model of the electric properties of the skin, are shown in figure 2.3

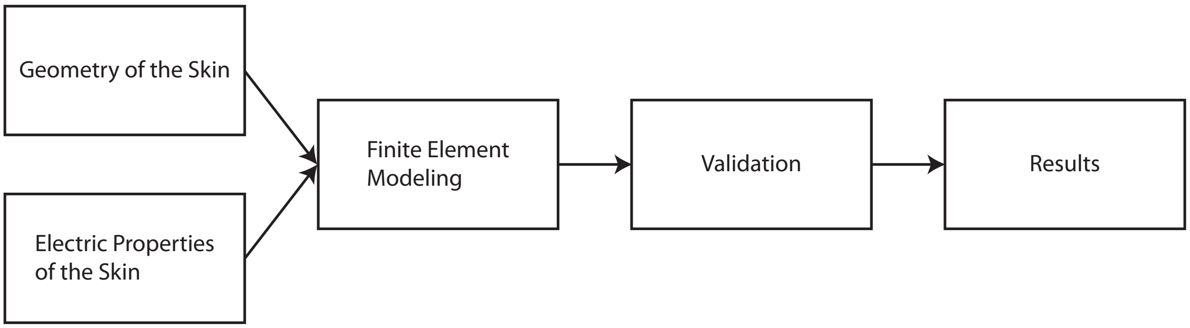

Figure 2.3: illustrates the steps conducted due to the development of the model of the electric properties of the skin

The knowledge that must be acquired prior to the modeling includes the physiology of the skin and a litteratur survey of studies measuring the thickness of the layers of the skin. This is found in chapter 3. In chapter 4 the theory regarding electric fields and electric material properties are outlined prior to a review of article examining the electric properties of the skin. After the preliminary analysis the actual modeling can be conducted. The design of the model based on the findings in the previous chapters is described in chapter 5 along with a description of finite element modeling and the implementation. The model is, hereafter, validated to determine whether the model of the electric properties of the skin behaves like the skin in vivo. This is done by comparing the impedance of the skin with the impedance found in the model. The comparison is conducted utilising different cathodes diameters in the concentric surface electrode described previously. After the model has been validated the resulting current flow is measured in order to substantiate the hypothesis. To verify that the finite element model calculates as expected a verification has been conducted and is presented in appendix A.

Preliminary Analysis

II

3 The layers of the skin

In order to model the electric properties of the skin it must be considered whether different parts of the skin have different properties. Thus, this chapter shortly reviews the physiology of the skin. Hereafter, the thickness of the layers is determined by a literature survey.

3.1 Skin physiolology

The skin can be divided into two major layers; epidermis and dermis. Besides these two layers a third layer, the hypodermis, is sometimes included in the description of the skin, even though it not actually is a part of the skin. Besides this the skin contains several different appendages such as hair, sebaceous glands and sweat glands.

3.1.1 Epidermis

The epidermis consists mainly of a continuous self-renewing, keratinized, stratified squamous epithelium. Keratinocytes are the most frequently appearing type of cell in the epithelium. Most of the remaining cells, termed non-keratinocytes, include melanocytes, Langerhans cells and lymphocytes. A third cell type, termed Merkel cells, is also present in the epidermis. The non-keratinocytes and the Merkel cells only contain very small amounts of keratin filament bundles [Standring 2005]. The epidermis is avascular, meaning that it does not contain blood vessels and is consequently relying on nutrients and oxygen from capillaries placed in the dermis [Martini 2004].

The population of keratinocytes undergoes continuous renewal throughout life. This occurs at the base of the epidermis and replaces the keratinocytes which simultaneously are shed to the surface. As they move outward they undergo various changes. Due to this, five different layers can be defined, corresponding to the progress of the change. From deep to superficial; basal layer (stratum basale), spinous or prickle cell layer (stratum spinosum), granular layer (statum granulosum), clear layer (stratum licidum) and cornified layer (stratum corneum). The three deepest layers are metabolic active through which the cells change their form as they progressively differentiate. In the two most superficial layers the cells undergo keratinozation also termed cornification. The cornification involves structural changes in the keratinocytes, alteration in the relationship with each other and with non-keratinocytes. Furthermore there are molecular changes within the intercellular space [Martini 2004], [McMahon & Kolzenburg 2006]. On figure 3.1 the different layers of epidermis are shown. It can be seen that the further the keratinocytes are shed towards the surface of the skin, the more flattened the cells become.

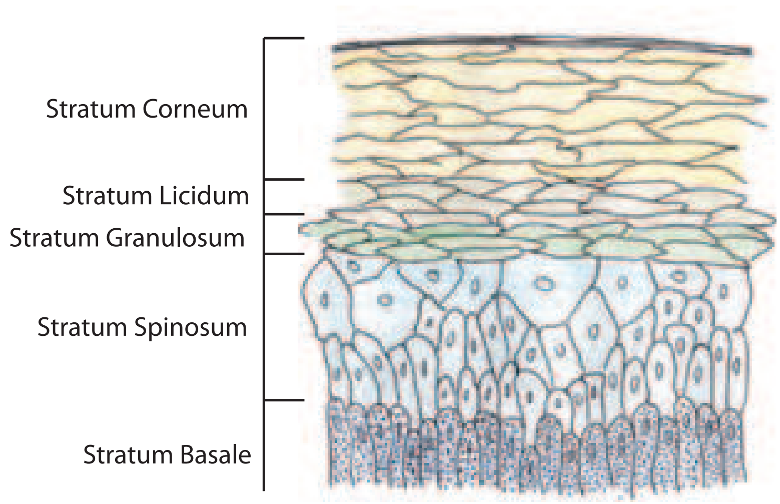

Figure 3.1: illustrates the layers of epidermis. Inspired by [Anne 2003].

The basal layer is the layer closest to the dermis and is, therefore, the layer which has the best access to nutrients and oxygen. To enable the best possible diffusion of nutrients and oxygen the stratum basale forms epidermal ridges extending into the dermis, increasing the area of contact between the two regions [Martini 2004], [Standring 2005]. The distinction between the electric properties of this layer and dermis are not pronounced.

When the keratinocytes reach statum granulosum, they have stopped dividing and begun making large amounts of the proteins keratin and keratohyalin. As keratin fibers are developed the cells become thinner and the cell membranes thicker, this prompt the cells to become less permeable. Keratohyalin forms dense granules in the cytoplasm; this promotes dehydration of the cell and aggregation and cross linking of the keratin fibers. In addition the nuclei and the other organelles in the cell disintegrate and finally cause the cells to die. Further dehydration creates a tight interlocked layer of cells that consist of keratin fibers surrounded by keratohylin [Martini 2004], [Standring 2005]. As the cell membranes become thicker the and the cells dehydrate the electric properties changes, i.e., the impedance increases.

The stratum corneum is the most diverging layer compared with the others. It consists of 15 to 30 layers of karatinised cells, but can be up to 50 cells deep. When the thickness of the skin increases, it is the number of cell layers in the stratum corneum, which increases. The cells in this layer are overlapping and interlocking with adjacent cells by ridges, grooves and microvilli [Martini 2004] [Standring 2005]. Due to the keratinisation the cells lacks a nucleus and membranous organelles. The stratum corneum does, therefore, only consist of a dense array of keratin filaments embedded in a cytoplasmic matrix which is partly composed of filaggrin derived from keratohyalin granules [Standring 2005]. The stratum corneum forms a protective barrier of dead, durable and expendable cells and its dry surface makes it unsuitable for growth of many microorganisms. Maintenance of this barrier involves coating the surface with lipid secretions from sebaceous glands. The layer is water resistant but not waterproof. This permits interstitial fluids to slowly penetrate the surface and afterwards to be evaporated into the surrounding air. This is in addition to the perspiration produced by the sweat glands [Martini 2004]. The electric properties of stratum corneum are the most diverging compared to the other layers of the skin. The impedance is very high due to the dryness of the cells the impedance becomes very high.

The melanocytes synthesize and store the pigment melanin, which gives the skin a dark color. The melanin protects the epidermis and dermis from the otherwise harmful effects of sunlight, which contains significant amounts of ultraviolet radiation. The melanocytes are located in the stratum germinativum [Martini 2004], [Standring 2005].

Langerhans cells are participating in the immune response and are responsible for stimulating a defense against microorganisms that manage to penetrate the superficial layer of the epidermis. Furthermore the Langerhans cells are responsible for stimulating of defense against superficial skin cancers [Martini 2004]. The Langerhans cells are regularly distributed throughout the basal and the prinkle cell layers and it appendages, except in the sweat glands [Standring 2005].

The Merkel cells are nerve cells and sensitive to touch and when they are compressed they release transmitter substances and thereby stimulate sensory nerve endings of Aβ fibers. The Merkel cells are primary found in the basal layer of epidermis. The Merkel cells are monitored by Merkel discs, which are located in the border area between the epidermis and dermis [Martini 2004]. This and the free nerve endings are the only kind of sensory receptor found in epidermis [Martini 2004], [Standring 2005]. On figure 3.2 the location of Merkel cells and free nerve endings can be seen.

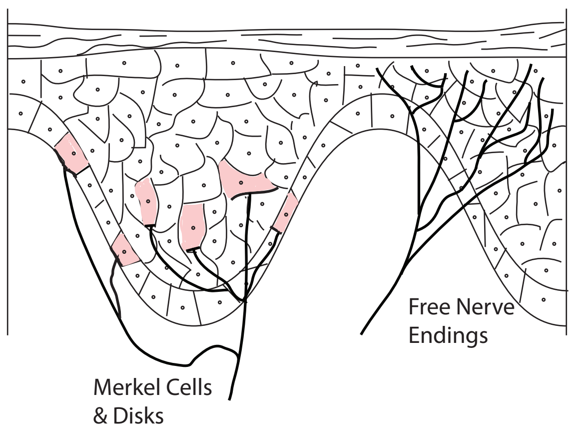

Figure 3.2: illustrates Merkel cells and free nerve endings. Inspired by [Martini 2004].

The Merkel cells are also found near large hair follicles in the dermis. The location entails that the Merkel cells respond to directional deformation of epidermis and direction of hair movement [Standring 2005]. Other types of sensory receptors are found in dermis [Martini 2004].

3.1.2 Dermis

The dermis is an irregular moderately dense connective tissue, composed of collagenous and elastic network in a ground substance of glycosaminoglycans, glycoproteins and bound water, which accommodates nerves, blood vessels, lymphatic epidermal appendages and a changing population of cells. Due to the virtue of the number and arrangement of the collagen and the elastic fibers, the dermis provides a considerable strength. The dermis consists of two layers which are visually indistinct; a narrow superficial papillary layer and a deeper reticular layer [Martini 2004], [Standring 2005].

The tissue in the papillary layer consists of fibers arranged in a mesh; besides these fibers this layer does also contain capillaries and sensory neurons. The reticular layer consists of an interwoven meshwork of dense, irregular connective tissue. Bundles of collagen fibers extend beyond the reticular layer and blend into the superficial papillary layer [Martini 2004].

The dominating categories of cells in dermis are permanent resident and migrant cells. The first mentioned include cells of organized structures such as nerves, vessels and cells of the arrector pili muscles and the fibroblasts, which synthesize all component of the dermal extracellular matrix. The migrant cells originate in the bone marrow and include macrophages, mast cells eosinophils, neutrophils, T and B cells and dermal interstitial dendritic cells, which are capable of immune surveillance and antigen presentation [Standring 2005].

Numerous different sensory organs are present in dermis, these includes both mechanoreceptors and thermal receptors. There are specific corpuscles and receptors responding to different types of mechanical touch, including; pressure, skin stretch, stroking and vibration [Kandel et al. 1991], [Martini 2004]. Most of these are $A\alpha$ and $A\beta$ fibers [Kandel et al. 1991].

3.1.3 Hypodermis

Besides the epidermis and the dermis, the hypodermis is sometimes considered a part of the skin. The boundary between the hypodermis and the dermis is generally indistinct. Hypodermis is important in stabilising the skin in relation to the underlying tissues, such as skeletal muscles or other organs, while permitting independent movement. The hypodermis consists of areolar and adipose tissues. The quantity of subcutaneous fat differs widely between body sites and is most abundant in the lower anterior abdominal wall [Martini 2004], [Standring 2005].

3.1.4 Skin Appendages

The most frequently appearing appendages are hair follicles, sebaceous glands and sweat glands

Hair is filamentous cornified structures present on almost the entire body surface. The skin is glabrous on the thick skin on the sides of the soles and on the palms of the hands, on the flexor surfaces of the digits and lips. The hair has a small function on the thermal regulation; this is primary on the scalp. Besides this they have a sensory function as sensory nerves surrounds the base of each hair follicle and responds to movement of the hair. The hair follicle is a down growth of the epidermis containing a hair, which may extend deeply into the hypodermis or may be more superficial within the dermis. The number of hair follicles varies widely with the body site [Martini 2004], [Standring 2005].

Together with the muscle that enables the hair to erect the sebaceous glands form what is called the pilosebaceous unit. They are present on the whole body except on the hairless skin of the palm, soles and flexor surfaces of digits, thus can be present in hairless skin [Standring 2005]. The gland cells produce a large quantity of lipids as they mature. The lipids released from gland cells enter the lumen or open passageway of the gland and are shed towards the surface of the skin e.g., by movement of the hair [Martini 2004]. The sebaceous glands functions as a protective coating of the hair and possibly helps waterprofing the epidermis [Standring 2005].

Besides the above appendages two types of sweat glands are present in the skin. The first type is among other places found in the armpits and secretes their product into the hair follicles. The other type is far more numerous and widely distributed. They are much smaller than the first mentioned type and does not extend as far into the dermis. The highest concentration is found in the palms and soles. Sweat consists 90 % of water and is chiefly a 0.1 t0 0.4 % saline solution of sodium chloride [Martini 2004].

On figure 3.3 an overview of the skin and it appendages are shown. The ridges mentioned earlier found in the transition between dermis and epidermis is also illustrated on the figure.

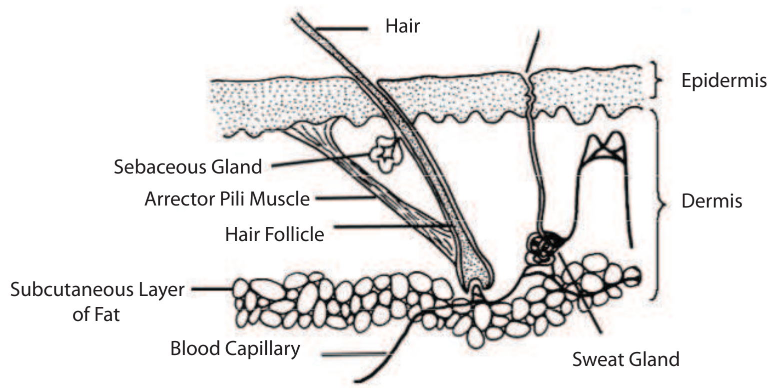

Figure 3.3: illustrates the skin and its main appendages [Lawson n.d.].

3.2 Thickness of layers of the skin

To ensure that realistic thicknesses of the skin are utilised in the model the following five articles regarding the thickness of the skin is reviewed; Sandby-Møller et al. [2003], Neerken, Lucassen, Bisschop, Lenderink & Nuijs [2004], Moore, Lunt, McManus, Anderson & Herrick [2003] and Yamamoto & Yamamoto [1976*a*], [1976*b*]. It is decided that the model of the electric properties of the skin should resemble the skin on the volar aspect of the forearm, since the majority of articles found examines this body site.

Sandby-Møller et al. [2003] examined the epidermal thickness and its relationship to age, gender, skin type, pigmentation, blood content, smoking habits and body site. The thickness was examined from biopsies taken from three different body sites in 71 human subjects. The subjects were between 20 to 68 years. The used skin was clinically normal skin. Three body sites were examined; the dorsal aspect of the forearm, the shoulder and the buttock.

A significant difference was found in the thickness between the different body sites for stratum corneum and the cellular epidermis, $p < 0.0001$A significant difference was also found between genders for both parts of the epidermis. The type of skin and pigmentation were only significant in relation to stratum corneum. Furthermore the blood content and the number of years smoking was only a significant factor in the cellular epidermis. However the findings done by Sandby-Møller et al. [2003] showed that the influence of body site exceed the inter-individual differences. The body site was capable of explaining 45 % of the variation in the measured thickness of stratum corneum and 39 % of the variation found in the cellular epidermis. The thickness of the dorsal aspect of the forearm found by Sandby-Møller et al. [2003] is given in tabel 3.1.

Neerken et al. [2004] examined the overall effect of aging skin derived from two different age groups; one consisting of volunteers between 19 and 24 years old and another consisting of volunteers in the age between 54 and 57 years. The mean age was 22.5 and 55.3 years for the two groups respectively. The origin of the examined skin was the volar aspect of the forearms and the temples. The skin was examined in vivo by using confocal laser scanning microscopy and optical coherence tomography. These two methods complement each other and thereby provide complementary information regarding the composition and structure of the skin; this is mainly due to the difference in their spatial resolution and penetration depth. By using two different techniques a more consistent interpretation of the images of the skin were obtained. The thickness of stratum corneum was determined as the depth at which a regular structure of cells were first visible, this is illustrated on figure 3.4. The minimum and maximum depth of the epidermis was determined by the top of the uppermost papillae and when there for the first time were no cellular structure observed respectively. The minimum corresponds to the part of the epidermis where there is no contribution by the dermis. This is illustrated on figure 3.4. The thickness of the cellular epidermis can be calculated as the mean of the maximum and minimum depth of epidermis minus the thickness of stratum corneum, as can be seen from figure 3.4.

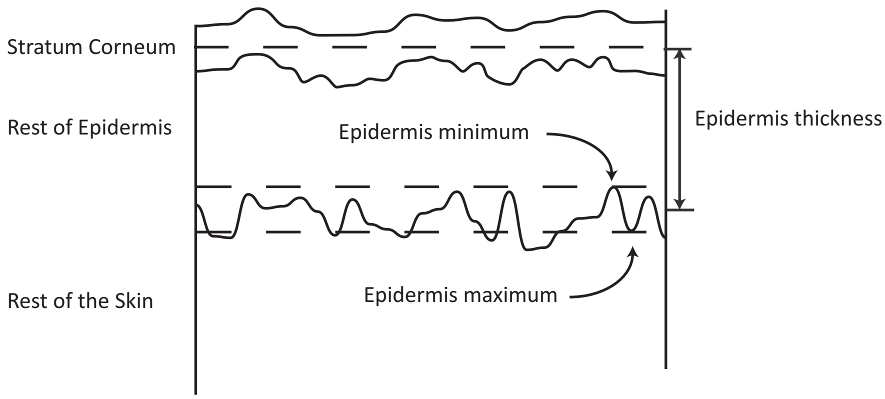

Figure 3.4: illustrates the depths and thicknesses found in [Neerken et al. 2004].

The thickness of the forearm found by Neerken et al. [2004] is given in tabel 3.1. Moore et al. [2003] examined the thickness of epidermis and dermis at seventeen different body sites in 39 patients with systemic sclerosis and in 34 healthy control subjects. Only the controls are of interest in this project. The control group consisted of 5 males and 29 females between 26 and 74 years, the median age was 47 years.

The skin thicknesses were found at the middle finger, dorsum, the volar aspect of the forearm and the upper arm, thigh, lower leg and foot. All measurements were conducted on both the left and the right side. In addition the skin thicknesses were found on the forehead, the anterior chest and abdomen. The skin thicknesses were measured with ultrasound. The thickness of epidermis and dermis were calculated after the surface epidermis, the epidermis-dermis and the dermis-hypodermis interfaces were found. In table 3.1 the thicknesses of epidermis and dermis are shown. In order to examine the electrical properties of stratum corneum Yamamoto & Yamamoto [1976*a*], [1976*b*] carried out a stepwise cellulose-tape stripping of the skin. After each stripping the thickness of the removed keratin layer was measured. A total of 15 strippings were performed on each subject. After this the subjects felt a touch of pain indicating that the stratum corneum is almost entirely removed and thus exposing the granular cell layer. The thickness of the stratum corneum was estimated to 40 μm. This finding is larger than in the aforementioned articles. Between each stripping an electrode was applied for a period of 30 minutes to stabilise, this may have moistened the skin and increased the thickness of the stripped layers. No information regarding the number of participating subjects was stated in the articles.

In table 3.1 the thicknesses of epidermis and dermis found in the studies conducted by Sandby-Møller et al. [2003], Neerken et al. [2004] and Moore et al. [2003] are shown.

	Epidermis [µm]		Dermis [µm]
Cite	Stratum Corneum	Cellular Epidermis	
Sandby-Møller et al.	18	57	-
Nerken et al.	29	40	-
Moore et al.	245		828

Table 3.1: shows the thicknesses of epidermis and dermis. Epidermis is separated into stratum corneum and the cellular part of epidermis [Sandby-Møller et al. 2003], [Neerken et al. 2004], [Moore et al. 2003].

Based on the above articles the thicknesses of the layers of the skin are determined. It was in the previous section outlined that the stratum corneum is the most distinct layer compared to the rest of the skin. Thus, it is chosen to utilise two layers in the finite element model; one layer resembling stratum corneum and one layer including both the cellular epidermis and dermis. The ridges found in the transition between epidermis and dermis is, thereby, not included in the model of the electric properties of the skin.

According to Sandby-Møller et al. [2003] the body site has great influence on the thickness of the stratum corneum and the cellular epidermis. It is, therefore, chosen to use the volar aspect of the forearm, for which the thickness has been found in all the reviewed articles.

The thickness of the layer resembling stratum corneum is calculated as the mean of the thickness found by Sandby-Møller et al. [2003] and Neerken et al. [2004]. The thickness of the remaining skin becomes the thickness of the dermis found by Moore et al. [2003] added with the mean of the thickness of the cellular epidermis found by Sandby-Møller et al. [2003] and Neerken et al. [2004]. The findings of Yamamoto & Yamamoto [1976*a*], [1976*b*] are disregarded.

It is chosen to disregard the presence of any appendages in the model, even though these are large contributors to the structure of the skin. This is done, due to findings in the next chapter, regarding the electric properties of the skin. The distribution of the appendages is, therefore, not further examined.

In figure 3.5 the skin as it appears in the model is shown.

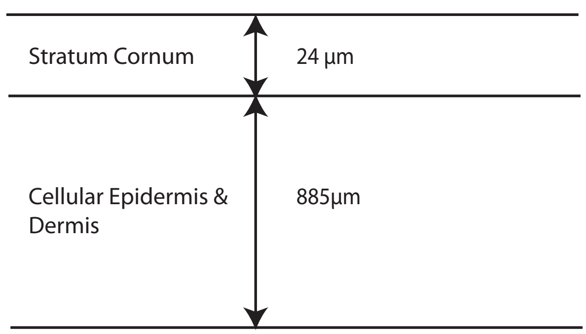

Figure 3.5: illustrates the layers of the skin, as it appear in the finite element model.

The electric properties of the skin 4

In relation to the development of a model of the electric properties of the skin, it is essential comprehend the theory of the electric fields and conducting and dielectric materials. Hereby, it becomes clear which equations it is necessary to solve in order to examine the distribution of the current density in the skin and a understanding of the electric properties are obtained. Hereafter, the electric properties of the skin are determined. This is done by reviewing studies which have experimentally and theoretically found the electric properties of the skin. In the following vectors are written in bold and fields are written in bold and by an over line.

4.1 Electric Fields

Electric forces are caused by electric charges. A charge can either be positive or negative. Charges with the same sign will repel each other whereas two charges of opposite sign will attracted each other. The force keeping two charges of same sign appart is given by Coulombs law:

$$\bar{\mathbf{F}}_{\mathbf{e}} = k_e \frac{|q_1||q_2|}{r^2}\,\hat{\mathbf{r}} \tag{4.1}$$

q_1 and q_2 are the magnitude of the two charges measured in Coulombs, r is the distance between the two charges, $\hat{\mathbf{r}}$ is a unit vector pointing in the direction from one charge to the other. k_e is the Coulomb constant which has been found experimentally by Charles Coulomb:

$$k_e = \frac{1}{4\pi\varepsilon} \tag{4.2}$$

where ε is a material property given by:

$$\varepsilon = \varepsilon_0\varepsilon_r \tag{4.3}$$

ε_0 is the permittivity of vacuum and equals approximately $10^{-9}/36\pi$ Farad per meter, F/m. ε_r is the relative permittivity of the material. The relative permittivity is dimensionless and larger than or equal to 1 [Ebert & Raskmark 1998], [Serway & Jewett 2004], [Grimnes & Øjran G. Martinsen 2000]. The interpretation of permittivity is further outlined in section 4.2.

An electric field is said to exist in the vicinity of a charged object. To be able to quantify the electric field a test charge is utilised. The electric field, $\bar{\mathbf{E}}$, is ,thereby, defined as the force exerted on a test charged placed in the electric field and is given by:

$$\bar{\mathbf{E}} = \frac{\bar{\mathbf{F}}_{\mathbf{e}}}{q_0} \tag{4.4}$$

The electric field is given in Newton per Coulomb, N/C, which is equal to volt per meter, V/m. The test charge is only placed in the electric field in order to enable the measurement of the size and direction of the electric field and is not a contributory cause to the electric field. It is therefore a necessity that the test charge is sufficiently small to ensure that the examined electric field is not influenced by the test charge. Equation 4.4 can be rewritten, to be able to better comprehend the concept of an electric field:

$$\bar{\mathbf{F}}_{\mathbf{e}} = q\bar{\mathbf{E}} \tag{4.5}$$

This equation expresses the force on a charge placed in an electric field [Ebert & Raskmark 1998], [Serway & Jewett 2004].

The electric field has both a magnitude and a direction and if equation 4.1 is inserted into equation 4.4 and one of the charges in equation 4.1 is the test source and the other is the charge from a point source, equation 4.4 becomes:

$$\bar{\mathbf{E}} = k_e \frac{q_{source}}{r^2}\,\hat{\mathbf{r}} \tag{4.6}$$

Visually the electric field can be shown as lines termed electric field lines as seen in figure 4.1.

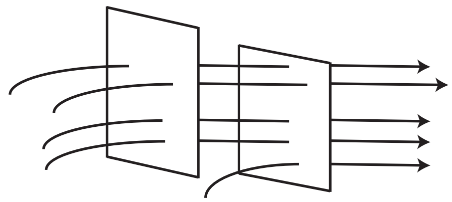

Figure 4.1: illustrates electric field lines. The surfaces perpendicular to the electric field lines illustrate surfaces utillised to calculate the flux density through the given region. Inspired by [Serway & Jewett 2004].

The electric field lines are tangent to the electric field vector at each point. The direction of the electric field is shown on the lines by arrowheads. The number of field lines penetrating a surface perpendicular to the lines is proportional to the magnitude of the electric field in that region, i.e., the closer the lines are together, the stronger the electric field and vice versa [Ebert & Raskmark 1998], [Serway & Jewett 2004].

The density of the electric field lines, termed the electric flux, Φ_E can be calculated by the following equation:

$$\Phi_E = EA \tag{4.7}$$

where E is the magnitude of the electric field and A is the area perpendicular to the field as seen on figure 4.1. The electric flux is given in $\mathrm{N} \cdot m^2/\mathrm{C}$. Equation 4.7 can be rewritten if the area approaches zero:

$$\Phi_E = \lim_{\Delta A_i \to 0} \sum E_i \cdot \Delta A_i \tag{4.8}$$

$$\Downarrow$$

$$\Phi_E = \int_{surface} \mathbf{E} \cdot dA \tag{4.9}$$

Equation 4.9 is a surface integral, meaning it must be evaluated over the surface in question. It is seen that the electric flux depends on both the pattern of the electric field and on the structure of the surface. If a electric point charge is located in the centre of a spherical closed surface, the electric flux through the sphere is given by:

$$\Phi_E = \frac{k_e q}{r^2}(4\pi r^2) \tag{4.10}$$

$$\Updownarrow$$

$$\Phi_E = 4\pi k_e q \tag{4.11}$$

$$\Updownarrow$$

$$\Phi_E = \frac{q}{\varepsilon_0 \varepsilon_r} \tag{4.12}$$

since the surface area of a sphere is $4\pi r^2$ and $k_e = 1/4\pi\varepsilon_0\varepsilon_r$. It can be shown that this can be applied to any closed surface also termed a gaussian surface [Ebert & Raskmark 1998], [Serway & Jewett 2004].

The material properties are not always constant, but can be inhomogen, anisotrop, nonlinear and time variant and it is, therefore, useful to be able to define the electric field independent of the these. Thus, another field termed the electric flux density, $\bar{\mathbf{D}}$ is defined:

$$\bar{\mathbf{D}} = \frac{q}{4\pi r^2}\hat{\mathbf{r}} \tag{4.13}$$

which equals:

$$\bar{\mathbf{D}} = \varepsilon\bar{\mathbf{E}} = \varepsilon_0\varepsilon_r\bar{\mathbf{E}} \tag{4.14}$$

The electric flux density is given in C/m^2

Another way of quantifying the electric field lines are by considering the charge density which is given in C/m^3:

$$\rho = \frac{dq}{dV} \tag{4.15}$$

The charge density considers the change in the charge in relation to the volume. This is equalent to the divergence, $\nabla\bullet$, of the electric flux density:

$$\nabla \bullet \bar{\mathbf{D}} = \rho \tag{4.16}$$

The above equation is termed Gauss' law of electricity and must be solved in order to examine the flow of the electric current applied to the skin [Ebert & Raskmark 1998], [Serway & Jewett 2004].

Gauss' law electricity is one out of four equations termed Maxwell's equation. Another relevant law is Maxwell-Ampères law which evaluates the link between electric fields and magnetism:

$$\nabla \times \bar{\mathbf{H}} = \mathbf{J} \tag{4.17}$$

where $\bar{\mathbf{H}}$ is the magnetic field strength in Ampere/meter and $\mathbf{J}$ is the total current density. $\nabla\times$ denotes the curl of the field. The total current density is the sum of three currents; the source current $\mathbf{J_s}$, the conduction current, $\mathbf{J_c}$, and the displacement current, $\mathbf{J_d}$.

The conduction current can according to Ohms law be written as:

$$\mathbf{J_c} = \sigma\bar{\mathbf{E}} \tag{4.18}$$

σ is the conductivity of the conducting medium, which is given in Siemens per meter, S/m, or alternatively 1/(Ohm · meter), $1/\Omega m$.

The displacement current can be written as:

$$\mathbf{J_d} = \varepsilon\frac{\partial\bar{\mathbf{E}}}{\partial t} \tag{4.19}$$

where $\varepsilon = \varepsilon_0\varepsilon_r$. Equation 4.17 thereby becomes:

$$\nabla \times \bar{\mathbf{H}} = \mathbf{J_s} + \sigma\bar{\mathbf{E}} + \varepsilon_0\varepsilon_r\frac{\partial\bar{\mathbf{E}}}{\partial t} \tag{4.20}$$

[Ebert & Raskmark 1998], [Serway & Jewett 2004]. The above equation is the equation, which must be solved in order to examine the distribution of the current density in the skin.

In order to solve equation 4.20 the link between electric fields and magnetism must be further evaluated, yet another of Maxwells equations must be taken into consideration; Faraday's law of induction:

$$\nabla \times \bar{\mathbf{E}} = \frac{\partial\bar{\mathbf{B}}}{\partial t} \tag{4.21}$$

which states that changes in a magnetic field, $\bar{\mathbf{B}}$, induces an electric field $\bar{\mathbf{E}}$.

The two material properties; conductivity and permittivity are examined in the following sections in order to get an interpretation of these before studies regarding these are reviewed.

4.2 Conducting and dielectric materials

In an electric conducting material some of the electrons are free, thus not bound to atoms and can therefore move relatively freely through the materials. In a perfect electric conductor the electrons can move effortless, thus there is no resistance [Serway & Jewett 2004]. A current density and an electric field are established in a conductor whenever a potential difference is maintained across the conductor. This is illustrated in figure 4.2.

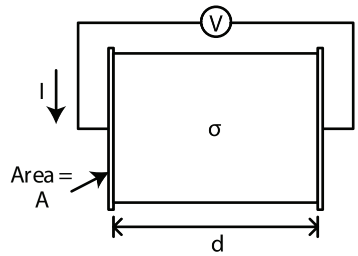

Figure 4.2: illustrates a conducting material held between a pair of electrodes on which a potential is applied. Inspired by [Reilly 1998].

The current density is given by:

$$\mathbf{J} = \frac{I}{A} \tag{4.22}$$

where A is the surface area of the electrodes. According to Ohms law given in equation 4.18 the established current density is proportional to the electric field:

$$\mathbf{J} = \sigma\bar{\mathbf{E}} \tag{4.23}$$

The potential difference is related to the field by the following equation, if the field is uniform:

$$\Delta V = Ed \tag{4.24}$$

where E is the magnitude of the electric field. Hereby, equation 4.23 becomes:

$$\mathbf{J} = \sigma\frac{\Delta V}{d} \tag{4.25}$$

Since the current density is defined as the current per unit area. The above equation can be rewritten to:

$$\frac{d}{\sigma \cdot A} = \frac{\Delta V}{I} \tag{4.26}$$

The left-hand side of equation 4.26 is the resistance, R, by which it can be defined as the ratio between the potential difference across a conductor and the current in the conductor. The current through the conducting material is can, thereby, by calculated by [Reilly 1998]:

$$I = \frac{\Delta V}{R} = \frac{\Delta V \sigma A}{d} \tag{4.27}$$

An ideal dielectric does, in contrary to a conductor, not contain any free charges; this corresponds to an insulator or a non-conductor. Figure 4.3 illustrates a non-conducting material held between a pair of parallel-plate electrodes on which a potential is applied.

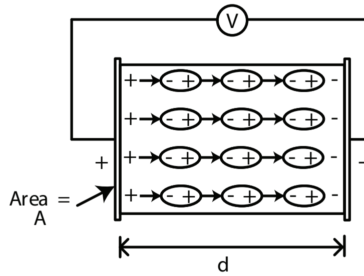

Figure 4.3: illustrates an ideal dielectric held between a pair of electrodes on which a potential is applied. The ovals are dipoles and the lines indicate electric flux lines. Inspired by [Reilly 1998].

There is no net current flow as response to the applied electric field since the material is non-conducting. Even though the material does not contain any free electrodes or ions the materials it is assumed to contain units of separated charge that are bound together into electrically neutral entities called dipoles. The displaced charge centers represent attractive forces within the dielectric medium, enhancing the internal electric field as indicated by the arrows in figure 4.3 [Reilly 1998].

The amount of charge, q, accumulated on the electrodes is directly proportional to the product of applied voltage, V, and capacitance, C, this gives:

$$q = C \cdot V \tag{4.28}$$

if the distance between the two electrodes is much smaller than its linear dimensions, thus the wavelength is much larger than the distance between the two electrodes, then the capacitance is given by:

$$C = \frac{\varepsilon_0 \cdot \varepsilon_r \cdot A}{d} \tag{4.29}$$

where A is the surface area of the electrodes, d is the distance between the electrodes. ε_0 is as aforementioned the permittivity of vacuum ($8.85 \cdot 10^{-12}$ F/m) and ε_r is the permittivity of the given material relative to ε_0. The permittivity is also termed the dielectric constant and ε_r can be interpreted as a measure of the materials ability to become polarized in response to an applied electrical field [Reilly 1998]. Polarisation can in general be defined as an electric field-induced disturbance of the charge distribution in a region. All materials are polarisable, the extent depends on the distribution of bound and free ions. If an electric field is applied to a material which only contains bound ions, the field does only displace the charges a small distance and this cause dipoles to be formed. A dipole is a doublet of two charges of opposite sign kept at a small distance and prevented from recombining. In an atom the electrons are at a distance from the positive nucleus, this does however not necessarily form net dipoles, since the electrical centre of the electrons may coincide with that of the nucleus. However it is possible to polarise all atoms, because the electrical centers of the charges will be displaced by an external electric field. Molecules may form permanent dipoles, these will however also be influenced by an externally applied electric field. When dipoles are formed they are said to be induced, this happens as positive and negative charges move in opposite directions. Induced dipoles are illustrated on figure 4.3. The polarisation, $\bar{\mathbf{P}}$, is on the more macroscopic level the dipole moment per unit volume [Grimnes & Øjran G. Martinsen 2000]:

$$\bar{\mathbf{P}} = \bar{\mathbf{D}} - \varepsilon_0 \cdot \bar{\mathbf{E}} \tag{4.30}$$

where $\bar{\mathbf{E}}$ is the electric field, as shown previously, and $\bar{\mathbf{D}}$ is the electric flux density or the displacement and is given by:

$$\mathbf{D} = \varepsilon_r \cdot \varepsilon_0 \cdot \mathbf{E} \tag{4.31}$$

by which equation 4.30 becomes:

$$\mathbf{P} = (\varepsilon_r - 1)\varepsilon_0 \cdot \mathbf{E} \tag{4.32}$$

The relationship between polarisation and permittivity is expressed in the above equation; high polarisation means high permittivity. Permittivity is thereby describing the amount of dipole moment density induced by an electric field.

The polarisation cannot itself be measured, and the theory regarding dielectric materials is therefore linked to the concept illustrated in figure 4.3, the capacitance can be measured and the polarisation calculated [Grimnes & Øjran G. Martinsen 2000]. Some molecules are as mentioned permanent dipoles, these are when not exposed to an applied electric field oriented randomly, however they will reorientate in the direction of the electric field when this is applied. Polar materials, i.e., materials containing permanent dipoles, have a higher permittivity than materials which does not contain permanent dipoles [Grimnes & Øjran G. Martinsen 2000]. The dipoles have a certain degree of inertia and will not be able to follow the field oscillation if it is too rapid. This entails that the permittivity is highest at low frequencies and falls when a certain frequency is reached. At very high frequencies the dipoles will be randomly orientated, by which the relative permittivity of the material will approach unity [Grimnes & Øjran G. Martinsen 2000], [Reilly 1998].

The current through an ideal dielectric is, therefore, time dependent:

$$I = C\frac{dV}{dt} = \frac{\varepsilon_0\varepsilon_R A\, dV}{dt} \tag{4.33}$$

Suppose the material between the two electrodes in figure 4.3 is not an ideal dielectric, then it is a partially conductor or a partially non-conductor and is defined by both the permittivity and the conductivity as illustrated on figure 4.4. The right side of the figure shows the equivalent electric circuit.

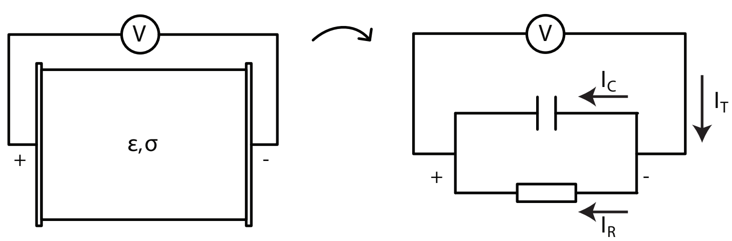

Figure 4.4: illustrates a non-ideal dielectric and its electric analogy. Inspired by [Reilly 1998].

The total current applied to the material is the sum of both the resistive and the capacitive components:

$$I_T = I_R + I_C \tag{4.34}$$

$$I_T = \frac{V}{R} + C\cdot\frac{dV}{dt} \tag{4.35}$$

where I_T is the total current, I_R is the current through the resistor, I_C is the current through the capacitor, V is the potential. If a sinusoidal AC current is applied and ideal conditions with no edge effects are assumed, then equation 4.35 becomes [Reilly 1998]:

$$I = \frac{V\cdot\sigma\cdot A}{d} + V\left(\frac{\varepsilon_0\cdot\varepsilon_r\cdot A}{d}\right)\cdot j\cdot\omega \tag{4.36}$$

This can be rewritten to:

$$J = \frac{j\cdot\omega\varepsilon_0}{d}\left(\varepsilon_r - \frac{j\cdot\sigma}{\omega\varepsilon_0}\right)\cdot V \tag{4.37}$$

Since the electric field and the current density are given by

$$\bar{\mathbf{E}} = \frac{\bar{\mathbf{V}}}{d} \tag{4.38}$$

$$J = \frac{I}{A} \tag{4.39}$$

respectively. The term in the parentheses in equation 4.37 is the complex permittivity which also can be written in another notation:

$$\varepsilon^* = \varepsilon' - j \cdot \varepsilon'' \tag{4.40}$$

in which ε' = ε_r and ε" = $\sigma/\omega \cdot \varepsilon_0$. The complex permittivity expresses the dielectric properties of a material, which also includes the losses [Grimnes & Øjran G. Martinsen 2000], [Reilly 1998], [Gabriel, Gabriel & Corthout 1996].

From the above derivation it has become clear that the permittivity is frequency dependent. Thus, the permittivity of the skin is also frequency dependent. The dielectric parts of the skin includes the cell membranes, thus, as the frequency becomes higher the current can pass through the membranes. This is illustrated on figure 4.5.

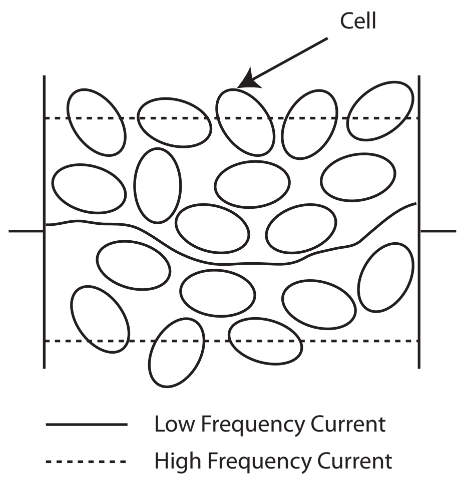

Figure 4.5: illustrates the current flow at high and low frequencies through a arbitrary tissue.

This means, that the current will flow through other materials when the frequency is low than when the frequency is high, and the conductivity of the skin does, thereby, also change when the frequency is changed [Grimnes & Øjran G. Martinsen 2000]. This is further elaborated in the following section.

4.3 Frequency dependence of the electric properties of the skin

To be able to utilise the permittivity to predict the pathways of the applied electric fields it is requisite to have knowledge about the frequency dependence of the permittivity. The frequency dependence can be explained by relaxation and dispersion and be presented by a Cole-Cole plot and equation.

4.3.1 Relaxation and dispersion

The permittivity is frequency dependent since the polarisation and displacement of charges in the material does not occur instantaneously, as described in the previous section. At low frequencies the charges have enough time to change position and polarisation will therefore be maximal at lower frequencies. At higher frequencies the polarisation and the permittivity will equivalently decrease. This time dependence is termed relaxation and occurs in the time domain. The relaxation time is denoted τ. The dispersion is the corresponding frequency depending permittivity; thus the permittivity as a function of frequency. In the simplest case the material has only one dispersion; one permittivity level at low frequencies when there is time for full relaxation and another lower level of permittivity at higher frequencies when there is not sufficient time to reach complete relaxation. The median value between to dispersion levels will occur at the characteristic frequency $f_c = 1/(2\pi\tau)$. In most materials there are more than one dispersion [Grimnes & Øjran G. Martinsen 2000], [Ørjan G. Martinsen, Grimnes & Schwan 2002]. In figure 4.6 idealised dispersion regions for a tissue are shown. In biological tissue these dispersions may be more or less pronounced [Ørjan G. Martinsen et al. 2002].

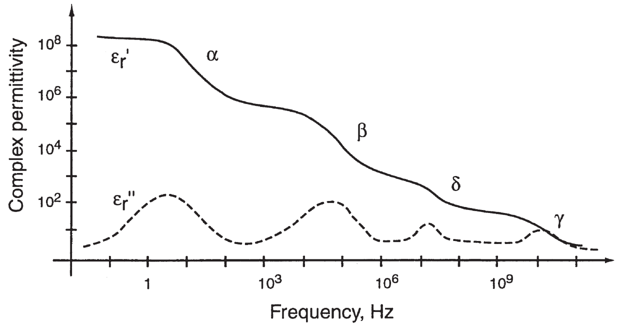

Figure 4.6: shows four idealised dispersions for a arbitrary tissue. The ε_r' and ε_r" is the real and imaginary part of the complex permittivity. α, β, δ and γ are different dispersions [Ørjan G. Martinsen et al. 2002].

In typical biological material there are at least three dispersions; α, β, and γ. Each of these are attributed different mechanisms of polarisation. The α dispersion is found at the lowest frequencies and is associated with ionic diffusion processes in the bilayers in organic molecules, ionic dispersion processes in micrometer-sized particles, active membrane conductance phenomena and other membrane effects. The β is related to the capacitive charging of the cellular membranes and the relaxation of proteins and other macromolecules. Finally the γ dispersion is attributed to the polarisation of water molecules [Reilly 1998], [Gabriel, Gabriel & Corthout 1996]. The two latter dispersions are found at radio and microwave frequencies respectively [Ørjan G. Martinsen et al. 2002].

4.3.2 Cole-Cole Equivalent Model

To present the frequency dependence of biological material a Cole-Cole plot can be utilised. A way to comprehend the Cole-Cole plot is based on an analogy of the cell membranes, intra- and extracellular fluids. The electric analogy is shown in figure 4.7(a). The cellular membranes are at low frequencies poor conductors but good capacitors, however, at higher frequencies the current will pass through the cell membranes and flow through the intracellular fluid as well. The frequency dependency of this circuit can be examined by generating a Cole-Cole plot which forms a circular arc, plotting the imaginary part of the impedance (the reactance) versus the reel part of the impedance (resistance). A Cole-Cole plot is obtained by measuring the resistance and reactance in a frequency sweep from zero to ideally infinity. The Cole-Cole plot for the electric circuit in figure 4.7(a) is shown in figure 4.7(b). It can be seen that at low frequencies the resistance is equal to R_1 and as the frequency reaches infinity the impedance becomes the parallel impedance of the R_1 and R_2; $R_1R_2/(R_1+R_2)$ [Foster & Lukaski 1996].

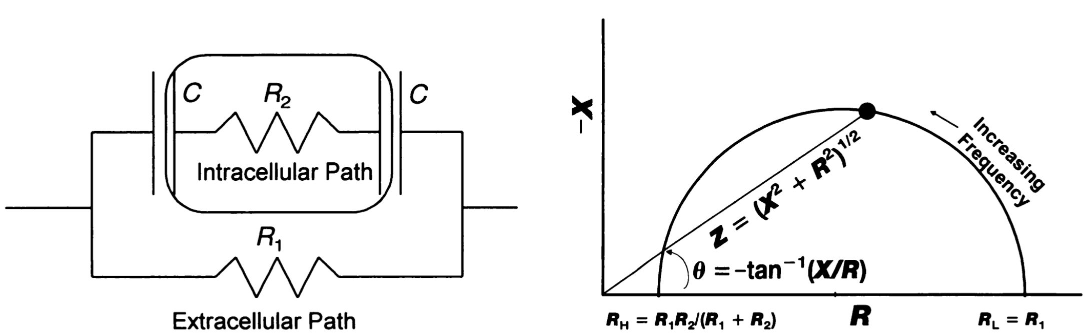

(a) (b)

Figure 4.7: (a) Shows an electric analogy of the intra and extracellular fluid. (b) shows a Cole-Cole plot of the electric circuit shown in (a) [Foster & Lukaski 1996]

The semicircle seen in figure 4.7(b) can be described by the following impedance function:

$$\mathbf{Z} = R_\infty + \frac{R_0 + R_\infty}{1 + (j\omega\tau)^\alpha} \tag{4.41}$$

Where the subscripts for R refer to the frequency, τ is a time constant, e.g., the mean relaxation time in a distribution of time constants, in addition 1 - α may be viewed as describing the width of the distribution of time constants. The Cole-Cole equation can also be written in terms of the permittivity:

$$\varepsilon(\omega) = \varepsilon_\infty + \frac{\Delta\varepsilon}{1 + (j\omega\tau)^{1-\alpha}} \tag{4.42}$$

where $\Delta\varepsilon$ is the difference between the permittivity at the stationary level at low frequencies and the permittivity at high frequencies at another level. The above equation is related to materials having only one dispersion. If there is more than one dispersion in the material, the spectrum of the tissue can more appropriately be described in terms the following equation, which also considers the conductivity [Gabriel, Lau & Gabriel 1996*b*]:

$$\varepsilon(\omega) = \varepsilon_\infty + \sum \frac{\Delta\varepsilon_n}{1 + (j\omega\tau_n)^{1-\alpha_n}} + \frac{\sigma_i}{j\omega\varepsilon_0} \tag{4.43}$$

If the geometries of the tissues are known, the permittivity can be calculated. By an equivalent method the conductivity can be determined.

4.4 Literature study regarding the electrical properties of the skin

There have been several attempts to determine the permittivity and conductivity of the skin in the last decades, e.g., by Yamamoto & Yamamoto [1976*b*] and [1976*a*], by Gabriel, Gabriel & Corthout [1996], Gabriel, Lau & Gabriel [1996*a*] and [1996*b*]. It is chosen only to review these articles since they encompass measurements of the material properties in vivo and in a broad frequency range.

In 1976 Yamamoto and Yamamoto wrote two articles regarding the electrical properties of the epidermal stratum corneum. In these the resistivity and dielectric constant of the epidermal stratum were determined by stripping the skin with cellulose-tape. The resistivity is the inverse of the conductivity [Reilly 1998]. The skin was stripped 15 times, the impedance measurement was conducted before the stripping begun and at intervals of three strippings, entailing a total number of six measurements. After the last stripping the measured resistivity and permittivity corresponded to that of the underlying layers of the skin. The measurement of the impedance was conducted with Ag-AgCl electrodes which were 9 mm in diameter on the ventral side of the forearm. The distance between the centers of electrodes was 50 mm. Electrode paste was used to ensure good electric contact. The electrodes were left on the skin in 30 minutes to stabilise before the measurement was conducted. Furthermore the polarisation impedance of the electrodes was measured, to be able to correct this in the measured impedance [Yamamoto & Yamamoto 1976*a*], [1976*b*].

The results of Yamamoto & Yamamoto [1976*a*] and [1976*b*] are presented as Cole-Cole plots in figure 4.8. 4.8(a) is an enlargement of 4.8(b).

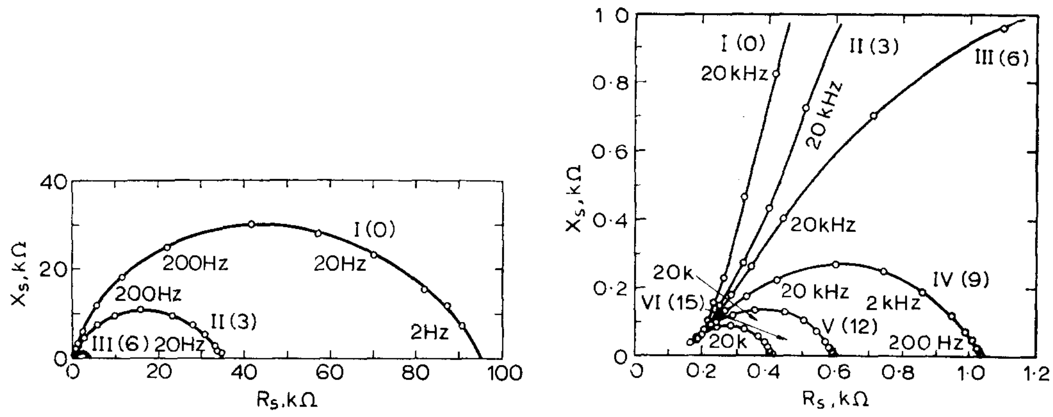

(a) (b)

Figure 4.8: shows Cole-Cole plots of the results from [Yamamoto & Yamamoto 1976*b*]. 4.8(a) is an enlargement of 4.8(b). The numbers in parentheses show the number of strippings with the cellulose tape, the Roman number tells the number of impedance measurement.

It was possible to calculate the resistivity (ρ) and relative permittivity of the stratum corneum and the rest of the skin by utilising equation 4.26 and 4.29 respectively, since the thickness of the stratum corneum was known in the experiment conducted by Yamamoto & Yamamoto [1976*a*] and [1976*b*]. The result is shown in figure 4.9.

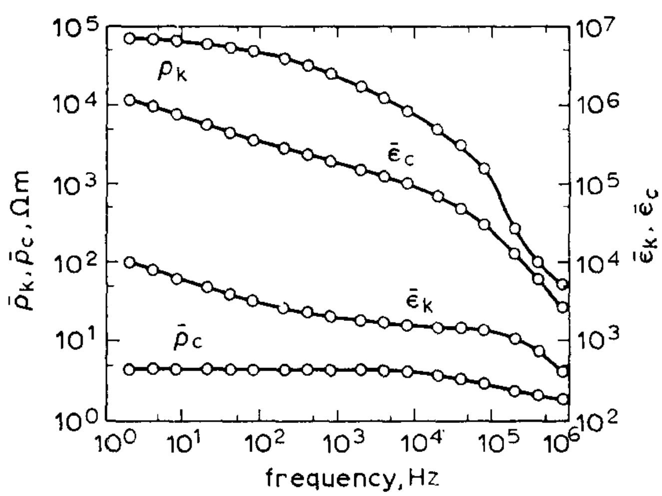

Figure 4.9: shows the resistivity (ρ) and relative permittivity (ε) found by Yamamoto & Yamamoto [1976*a*] and [1976*b*]. The subscribt k indicates the keratin layers of the skin, i.e., stratum corneum, whereas the subscript c indicates the rest of the skin.

The number of subjects on which the measurements were conducted was not stated in the either of the two articles. Furthermore, it is unfortunate that the electrodes are left on for 30 minutes to stabilise this have caused the electrode paste to interact with stratum corneum and probably increased the conductivity and maybe also the thickness of the skin, this would however have decreased the calculated conductivity and increased the calculated permittivity.

In 1996 three articles were published by Gabriel, Gabriel & Corthout [1996], Gabriel, Lau & Gabriel [1996*a*], Gabriel, Lau & Gabriel [1996*b*]. All three articles focus on different aspects regarding the dielectric properties of biological tissue; a literature survey, a measurement of the permittivity in the frequency range from 10 Hz to 20 GHz of various tissues and a calculation of parametric models of the dielectric spectrum of various tissues, including the skin. The two last-mentioned are of most interest in this section.

Gabriel, Lau & Gabriel [1996*a*] made an experimental study of various biological tissues including in vivo measurements of skin. The study used swept frequency techniques and measured the dielectric properties in the frequency range from 10 Hz to 20 GHz. Three different techniques were used, to ensure overlap of the frequencies and to demonstrate consistensy of the measurements. The results obtained from human skin are shown in figure 4.10. Nothing was stated in the article regarding removal of the stratum corneum; therefore, it is presumed to be a measurement of both the stratum corneum and the viable layers. The experimental data found by Gabriel, Lau & Gabriel [1996*a*] was in the range of the information found in the literature reviewed by Gabriel, Gabriel & Corthout [1996].

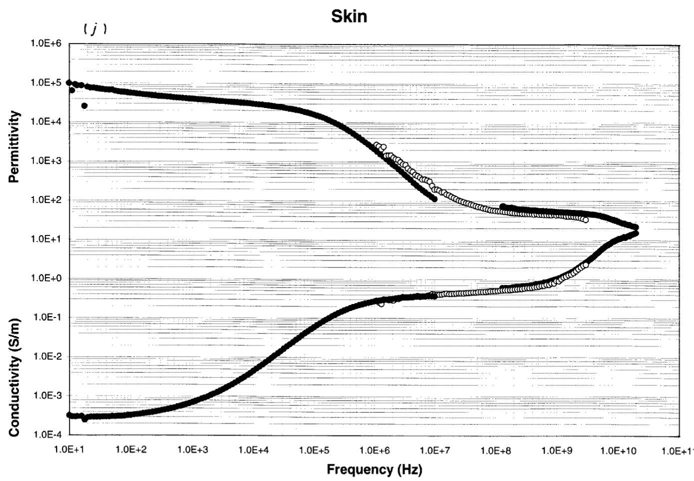

Figure 4.10: shows conductivity and permittivity measured by Gabriel, Lau & Gabriel [1996*a*]. The different markers indicate the different measurement techniques.

The number of participants was as in the articles publised by Yamamoto & Yamamoto [1976*b*] and [1976*a*] not specified. In addition the body site was not specified.

Lahtinen, Nuutien & Alanen [1997] commented on the findings of Gabriel, Lau & Gabriel [1996*a*]. They stated that it was questionable for which part of the skin the permittivity and conductivity was found. Hence, as the hypothesis of this project, they assert this depends on the size of the measuring electrodes. This means that it is not known whether the found permittivity and conductivity reflect the electric properties of the stratum corneum, the dermis or the subcutaneous layers. Gabriel [1997] argues against this by comparing the dispersions seen in figure 4.10 to the dispersions expected in stratum corneum and dermis respectively; The dermis contains blood vessels, sweat glands and other structures and is expected to exhibit dielectric behavior of a high-water-content tissue whereas the stratum corneum consists of layers of flattened, dead cells with almost no aqueous extra cellular fluid. Based on this no polarisation mechanisms originating from ionic displacement are expected to occur in stratum corneum. This is also the case in the measured permittivity seen in figure 4.10. Hence it can, according to Gabriel [1997], be concluded that the measured permittivity dominantly originates from the uppermost layers of the skin.

Gabriel, Lau & Gabriel [1996*b*] made a parametric model to be able to express the frequency dependence of the permittivity and conductivity. This was done for several tissues including the skin. It was chosen to estimate the parameters in equation 4.43 in up to four dispersions when requisite, meaning that the following parameters was estimated: ε_∞, $\Delta\varepsilon_{1-4}$, τ_{1-4}, α_{1-4} and σ. The numerical least-squares minimisation techniques was used to obtain the best estimate of the parameters. The analysis presented in the paper was based on the experimental data presented by Gabriel, Lau & Gabriel [1996*a*], complemented by the data surveyed from the literature by Gabriel, Gabriel &

Corthout [1996]. Only two dispersions were needed for the skin. The result obtained from the parametric model is shown on figure 4.11.

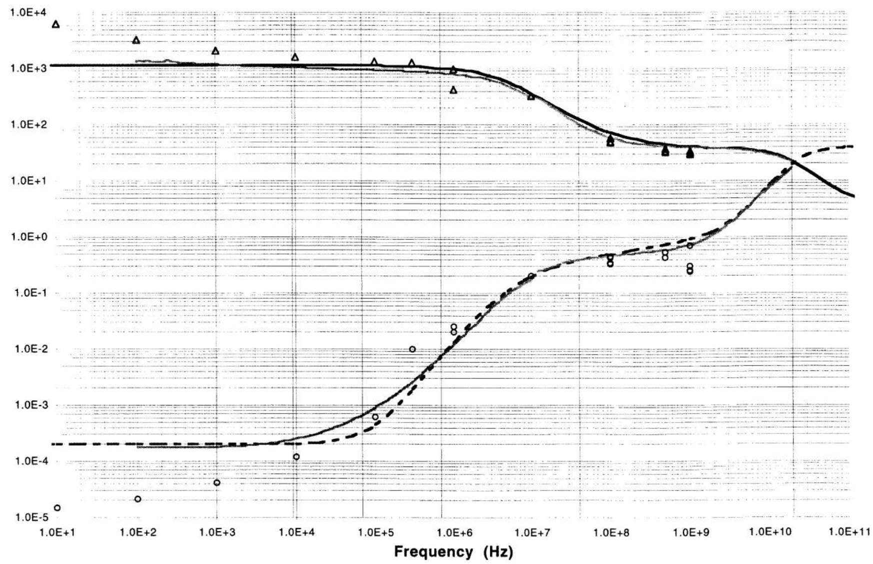

Figure 4.11: shows permittivity and the conductivity in the frequency spectrum for skin, when the result from the parametrisation is used. The black filled and dotted curves correspond to the permittivity and conductivity obtained due to the parametric model, whereas the triangles and circles indicate data from the litterature [Gabriel, Lau & Gabriel 1996*b*].

In the survey no studies were found, which solely examines the permittivity of the cells of either stratum corneum nor the rest of the skin. Thus, the layers of the skin have in all studies been regarded as one substance and appendages as hair and sweat glands have been ignored. This, even though, it is commenly known, that the current preferentially flows through the low-resistance skin appendages when possible [Reilly 1998], [Grimnes & Øjran G. Martinsen 2000], [Sha, Kenney, Heller, Barker, Howard & Moatamedi 2008]. This prompts that model designed in this project also considers the layers of the skin as one continuous mass.

The layers of the skin are as it became apparent in the description in section 3.1 not uniform. However there is in the survey of literature not found any studies handling the both the conductivity and permittivity of the skin in various directions in vivo. As a consequence the skin is assumed homogeneous.

The problem pointed out by Lahtinen et al. [1997] regarding which part of the skin the material properties are found, is not of concern in the study conducted by Yamamoto & Yamamoto [1976*b*] and [1976*a*]. Since Yamamoto & Yamamoto [1976*b*] and [1976*a*] made a comparative study where they gradual removed layers of stratum corneum while simulataneously measuring the skin impedance. Hence, they were able to determine the contribution from the removed skin. This entails that the material properties found by Yamamoto & Yamamoto [1976*b*] and [1976*a*] are applied in the model. More over the measurements done by Yamamoto & Yamamoto [1976*b*] and [1976*a*] was conducted on the same body site, as the data regarding the thickness of the layers of the skin.

In table 4.1 readings from figure 4.9 are shown. It is chosen to read the electric properties at different frequencies since they changes due to dispersions.

	Stratum Corneum				Rest of the Skin			
Frequency	10	100	1000	10000	10	100	1000	10000
ρ [Ωm]	$6 \cdot 10^4$	$4 \cdot 10^4$	$2 \cdot 10^4$	$8 \cdot 10^3$	5	5	5	5
σ [S/m]	$\mathbf{2 \cdot 10^{-5}}$	$\mathbf{3 \cdot 10^{-5}}$	$\mathbf{5 \cdot 10^{-5}}$	$\mathbf{1 \cdot 10^{-4}}$	**0.2**	**0.2**	**0.2**	**0.2**
$\boldsymbol{\varepsilon_r}$	$\mathbf{5 \cdot 10^3}$	$\mathbf{3 \cdot 10^3}$	$\mathbf{2 \cdot 10^3}$	$\mathbf{2 \cdot 10^3}$	$\mathbf{8 \cdot 10^5}$	$\mathbf{4 \cdot 10^5}$	$\mathbf{2 \cdot 10^5}$	$\mathbf{1 \cdot 10^5}$

Table 4.1: shows the permittivity and the conductivity read from figure 4.9 at the frequencies; 10, 100, 1000 and 10.000 Hz.

Ideally the properties should only be utilised if the environmental conditions are as when the study was conducted, this is however not possible to obtain. In addition, the same electrode paste should be utilised and the electrodes should be left on in 30 minutes as done in the study. However, due to the thesis statement of this project and the utilised electrodes, this is not doable. It must just be kept in mind that the conductivity found by Yamamoto & Yamamoto [1976*b*] and [1976*a*] might be larger, than when the concentric surface electrode utilised in this project is applied.

Solution

III

Finite Element Modeling 5

Based on the findings in the previous chapters, it is now possible to create a finite element model of the electric properties of the skin. Finite element modeling was developed in order to solve various partial differential equations in complex structures and has its origin in structural analysis of aircrafts. Since then, it has been applied to various applications, including electromagnetics. The finite element method has a high geometrical adaptability and has low memory requirements. It is, therefore, one of the most popular numerical methods in all branches of engineering [Volakis, Chatterjee & Kempel 1998].

The steps in finite element modeling are described in this chapter along with the development of the model. The development requires that some resolution are made, the reasoning behind are included in this chapter.

The finite element model is developed in the simulation environment COMSOL Multiphysics 3.5, referred to as COMSOL in the remaining of this chapter. The implementation is illustrated by screen shots from COMSOL.

Finite element modeling consists of five main steps; Selection of law of physics, Drawing of the geometry, Setting of material properties, boundary conditions and initial conditions, Meshing and Solving. The steps are illustrated in figure 5.1.

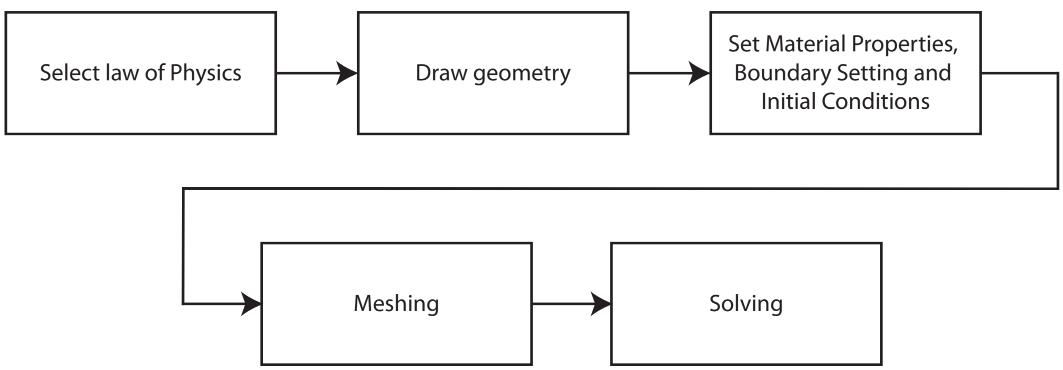

Figure 5.1: illustrates the processes that must be conducted when creating a finite element model

The first four steps are described in the following sections.

5.1 Selection of law of physics

The first step is to decide in which module the model should be developed. COMSOL is a multiphysics simulation tool, i.e., it has many different application modules including; acoustics, heat-transfer, fluid dynamic and electromagnetic. The choice of application module in which the model must be developed is based on the law of physics it must obey and whether any approximations can be made.

In order to examine the electric behavior of the skin due to an applied current the *AC/DC Module* is chosen. Maxwell-Ampères law given in equation 4.20 on page 25 is solved in this application. In addition it is chosen to use the *Quasi-Static Electric Approximation*. This approximation can be utilised when small currents are applied and when there are a negligible coupling between the electric and magnetic fields. In the following section the use of the quasi-static approximation will be justified and Maxwell-Ampères law will be adjusted due to the approximation.

The quasi-static electric approximation can be utilised, when the studied geometries are considerable smaller than the wavelength and when time variations are small. The changes in the electric field are not synchronised with the changes of the source, since the propagation of the electric field is finite. However, if the wavelength is sufficiently larger than the geometry the changes in the electric field appears small and the electromagnetic field can be considered stationary at every instant, i.e., the quasi-static electric approximation can be utilised [Multiphysics 2008]. This is illustrated on figure 5.2.

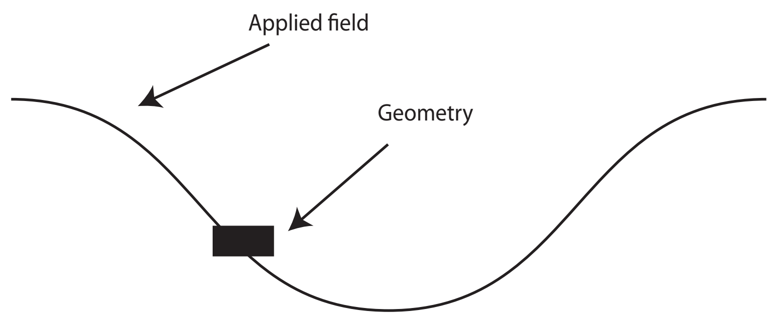

Figure 5.2: illustrates a small geometry, to which a field is applied. The wavelength of the applied field is much larger than the geometry.

To evaluate whether the geometry is sufficiently small it can be compared to the wavelength in the medium and the exponential attenuation of the wavefield. The exponential attenuation of the wavefield is the length were the signal is attenuated e^{-1}. The wavelength, λ, and the exponential attenuation, δ, is given by [Dewarrat, Falco, Talary, Feldman & Puzenko 2008], [Ebert & Raskmark 1998]:

$$\lambda = 1/\mathrm{Re}(k_c) \tag{5.1}$$
$$\delta = 1/\mathrm{Im}(k_c) \tag{5.2}$$

where k_c is the complex wavenumber, which is given by [Dewarrat et al. 2008], [Ebert & Raskmark 1998]:

$$k_c = \frac{\omega}{c}\sqrt{\mu\varepsilon^*} \tag{5.3}$$

where ω equals $2\pi f$, c is the velocity of light, μ is the relative magnetic permeability and ε^* is the complex permittivity as given in section 4.2 on page 25:

$$\varepsilon^* = \varepsilon_r - j \cdot \frac{\sigma}{\omega \cdot \varepsilon_0} \tag{5.4}$$

The relative magnetic permeability of the skin is assumed to be equal to 1. The wavelength and the exponential attenuation thereby becomes [Dewarrat et al. 2008], [Ebert & Raskmark 1998]:

$$\lambda = \frac{c}{\omega \mathrm{Re}(\sqrt{\varepsilon^*})} \tag{5.5}$$
$$\delta = \frac{c}{\omega \mathrm{Im}(\sqrt{\varepsilon^*})} \tag{5.6}$$

The wavelengths and exponential attenuations are calculated for the readings given in table **??** on page **??** and are shown in table 5.1. The frequency used in the calculation corresponds to the frequency at which the electric properties of the skin were read.

	Stratum Corneum				Rest of the Skin			
Frequency	10	100	1000	10000	10	100	1000	10000
λ [m]	$3 \cdot 10^4$	$7 \cdot 10^3$	$1 \cdot 10^3$	$1 \cdot 10^2$	356	112	35	10
δ [m]	$4 \cdot 10^4$	$1 \cdot 10^4$	$5 \cdot 10^3$	$2 \cdot 10^3$	356	113	37	13

Table 5.1: shows the calculated wavelengths and exponential attenuations based on the electric properties of the skin at different frequencies

The smallest length found was 10 meters, as seen in table 5.1. This must be compared to the dimensions of the developed model. The thickness of the layers of the skin was in chapter 3 page 15 found to be 909 μm. The diameter of the utilised surface electrode is 4 cm. The large difference between the dimensions of the model and the smallest found length justifies the utilisation of the quasi-static approximation.

Maxwell-Ampères law, which describes the propagation of applied current in a medium, can be simplified when the quasi-static approximation is assumed. The quasi-static approximation implies that the induced currents can be neglected. Thus;

$$\frac{\partial B}{\partial t} = \nabla \bullet \bar{\mathbf{E}} = 0 \tag{5.7}$$

that is, the divergence of the electric field becomes zero and the electric field can, therefore, be expressed in terms of only the electric potential. The electric field, thereby, equals [Multiphysics 2008], [Serway & Jewett 2004], [Ebert & Raskmark 1998]:

$$\bar{\mathbf{E}} = -\nabla V \tag{5.8}$$

By appling the divergence on both sides of Maxwell-Ampères law and inserting the electric field from equation 5.8 is becomes:

$$\nabla \mathbf{J_e} = \nabla(\mathbf{J_s} - (\sigma + \varepsilon_0 \varepsilon_r i\omega)\nabla V) \tag{5.9}$$

since the time derivative of the electric field is:

$$\frac{\partial \bar{\mathbf{E}}}{\partial t} = -i\omega \bar{\mathbf{E}} \tag{5.10}$$

The term $\nabla \mathbf{J_e}$ denotes the free charges in the medium.

The modified Maxwell-Ampères law given in equation 5.9 is the equation solved in the finite element model examining the electric properties of the skin.

The frequency of the applied current does, due to the definition of the quasi static approximation, not influence the calculation of equation 5.9. Hence, the solution will not change regardless of which frequency the applied current has. Thus, the result will only be correct if the wavelenght of the applied current is much smaller than the dimensions of the geometry.

5.2 Drawing of the geometry

In this step the model is drawn. This includes both the electrodes and the geometry of the skin.

The skin is a three dimensional structure, but in order to simplify the model this can be reduced to a two dimensional model by revolving a cross section around an axes. This entails that no variations occurs the around the axes.

Thus, the drawing is done in *2D axial symmetry*. This implies that the skin is modeled with cylindrical coordinates (r,z) where r = 0 is the revolution axis. This can be done due to symmetry in the model. A illustration of the model is shown on figure 5.3.

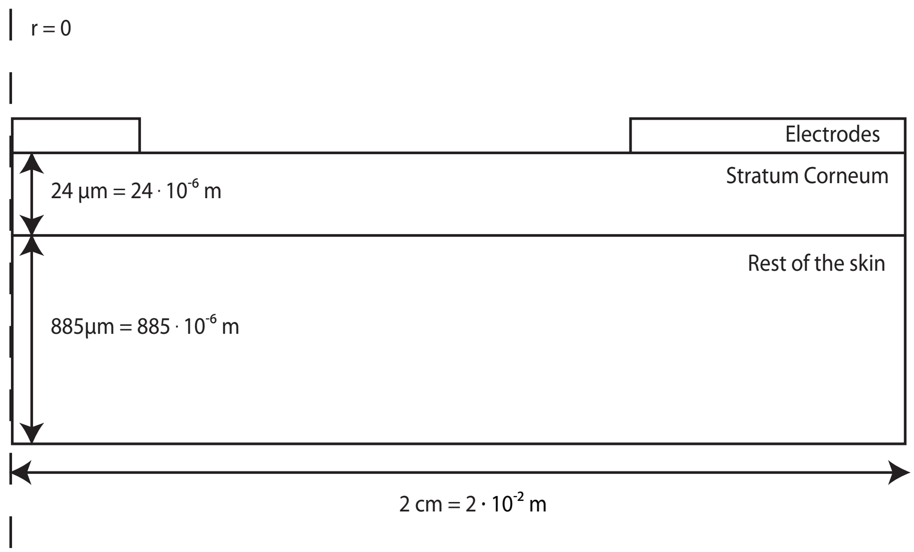

Figure 5.3: illustrates the drawing of the model of the skin and its dimensions

The dimensions of the model are given on figure 5.3. The transition between the stratum corneum and the rest of the skin, is modeled as a straight line, since the inter-variance among individuals is great and it is, therefore, not possible to settle for any specific structure.

The horizontal extent of the model is set to 2 cm; which is the same as the electrodes. This is considered as sufficient since the largest current density is between the two electrodes and the area of interest will, therefore, not include the area on the opposite site of the anode.

Figure 5.4 shows a part of the model drawn in the COMSOL.

5.3 Setting of material properties, boundary conditions and initial conditions

After the model has been drawn, the material properties, boundary conditions and initial conditions can be set.

The material properties of stratum corneum and the rest of the skin were determined in chapter 4. It was seen that both the permittivity and conductivity depended on the frequency. Thus, the electric properties of the skin must be changed, according to the frequency of the current, which it is desired to simulate. It must be stressed that the actual frequency of the current applied to the model does not need to correspond to the frequency at which the electric properties were found. This is due to the quasi static approximation.

The boundary conditions are set to insulators, i.e., the current through these are zero, due to the same assumption as in relation to the horizontal extent of the model.

No initial conditions are set, since the skin is not polarised when an electric field is not present. In addition no currents are presumed to present inside the skin, those who are are neglected.

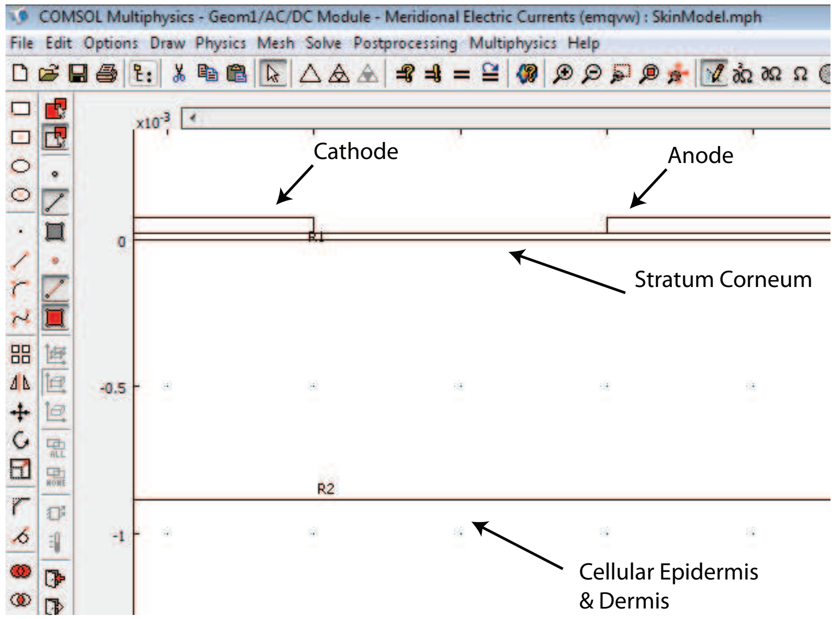

Figure 5.4: shows a part of the drawing of the model in COMSOL.

5.4 Meshing

Before the solving can be begun, a mesh is created in the drawn geometry. This is also termed discretisation and is illustrated in figure 5.6. This mesh divides the regions of the drawing into non-overlapping finite elements. The meshing should be considered as an interpolation exposing the variations inside the geometry. Thus, instead of the considering the geometry as one big element, it is divided into finite elements of arbitrary domain geometries, in the case shown on figure 5.6; triangles. A solution to Maxwell-Ampères law given in equation 5.9 are found for each of lines in the mesh

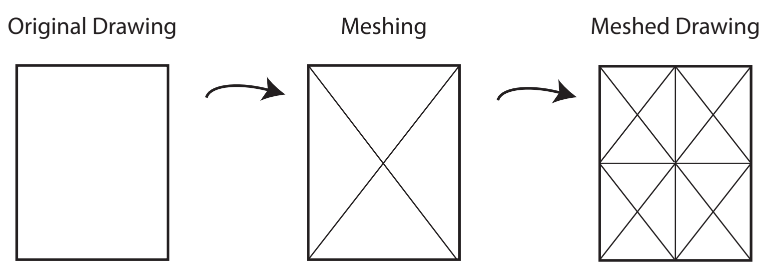

Figure 5.5: illustrates the concept of meshing. Maxwell-Ampères law is solved for each of the boundaries in the mesh instead of only at the borders.

On figure **??** the drawing of the model of the electric properties of the skin has been meshed.

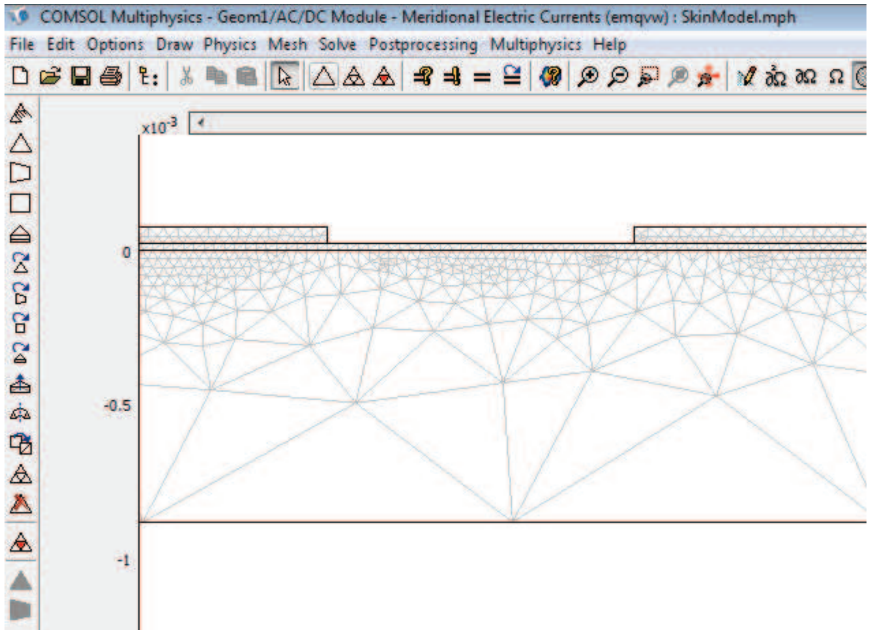

Figure 5.6: shows the drawing of the model in COMSOL after it has been meshed.

After the meshing has been conducted the solving can begin.

Validation 6

It must be ensured that the model of the electric properties of the skin resembles the human skin, in order to rely on the results obtained. Hence, a validation is conducted by comparing the impedance measured in the developed model, with the impedance measured on the skin. The validation was conducted with concentric surface electrodes introduced in chapter 2. Anodes with different diameters were utilised; 0.2, 4.0, 8.0, 12.0 and 20.0 *mm*.

The measurement of the skin impedance was conducted with equipment developed by Yoshida, Inmann & Haugland [1999]. Low amplitude broadband current waveform are injected through the utilised electrodes. The injected current and the resulting voltage waveforms are digitally sampled for 20 seconds. Both signals are Fast Fourier transformed and the complex Fourier coefficients of the voltage waveforms are divided by those of the current waveform to derive the complex impedance. The measurements were conducted on proximal part of both the right and the left forearm on one subject. The electrode was kept gently in place by a ribbon wrapped around the arm.

The impedance of the finite element model was calculated by applying a current to the anode and monitoring the voltage. After an electrode has been drawn in the model, a mesh must be developed inside the complete geometry consisting of the two layers of the skin, the anode and the cathode. Subsequently the solving can be conducted for the given geometry with the specified electric properties. It is possible to apply probes in order to monitor the electric potential and current in the model. The probes were placed in the middle of the anode. The impedance was measured at the frequencies; 10, 100, 1000 and 10000 Hz. The resulting impedance does, as described in chapter 5, not depend on the applied waveform, due to the quasi-static approach. Thus, it is the electric properties found at the different frequencies that determine the impedance and not whether the applied current has a frequency of 10 or 100 Hz.

The calculated impedances are shown in figure 6.1 and 6.2 for the study of the impedance on skin and for the model of the electric properties of the skin respectively. The impedance shown in figure 6.1 is obtained by measuring on the right forearm.

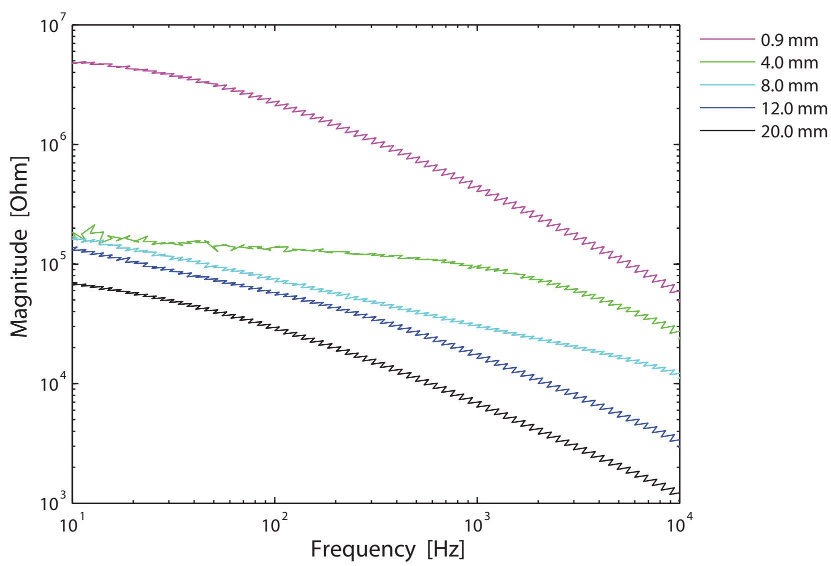

Figure 6.1: shows the impedance measured on the right arm in the frequency range from 10 to 10.000 Hz. The legends correspond to the diameter of the utilised anode.

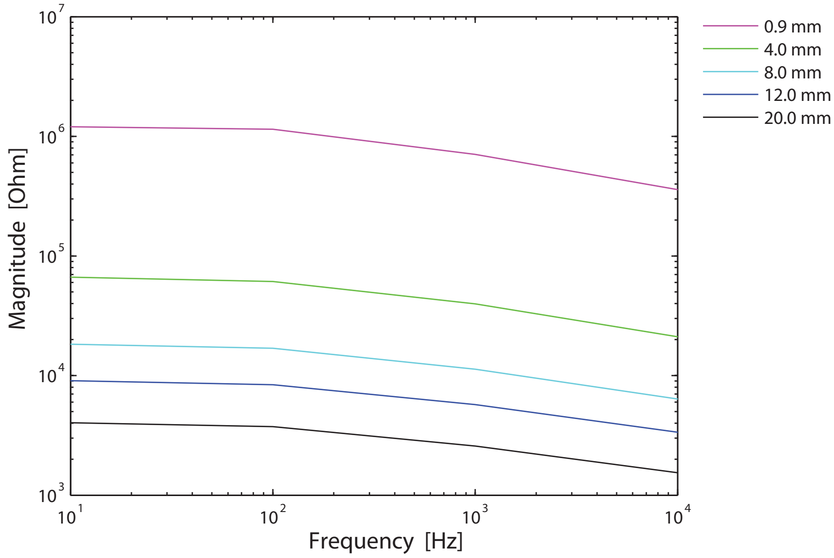

Figure 6.2: shows the impedance measured in the model in the frequency range from 10 to 10.000 Hz. The legends correspond to the diameter of the utilised anode.

The impedance found in the developed finite element model shows the same characteristics as the impedance measured in vivo. I.e., the measured impedance is higher when smaller electrodes are utilised than when larger electrodes are utilised. The impedance is, though, in general, smaller in the developed model, than in the real skin. At 10 kHz the impedances does, however, tend to converge.

Results 7

Concentric surface electrodes with different diameters are utilised to reveal whether the size of the concentric surface electrodes influences the flow of current in the skin. In order to test the hypothesis it must, in addition, be examined whether changes in distance between the anode and the cathode alters the distribution of the current density, since the distance between the two electrodes changes when the diameter of the anode changes. The electric properties of the skin change when the frequency changes and it is, therefore, examined whether the results change when the electric properties found at different frequencies are utilised.

When an electrode has been drawn in the model, a mesh must be developed inside the complete geometry consisting of the two layers of the skin, the anode and the cathode. Subsequently the solving can be conducted for the given geometry with the specified electric properties. A wide range of information can be obtained after the solving has finished. This includes the current density. The distribution of the current density in the geometry can be visualised in a surface plot. An example is shown in figure 7.1.

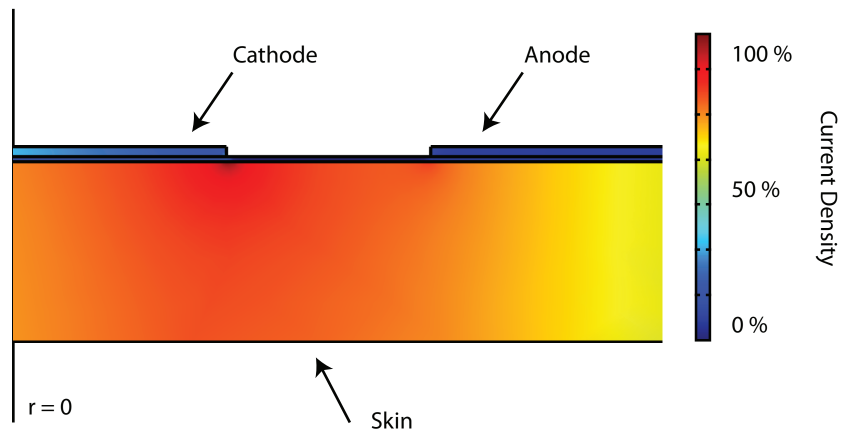

Figure 7.1: shows a part of a surface plot of the distribution of the current density in the model of the electric properties of the skin

Probes are used to quantitatively monitor the distribution of the current density at different depths in the model. The probes are placed in ten columns between the anode and cathode. Five of the columns are equally distributed between the outer edge of the cathode and the inner edge of the anode. The distance between these columns changes when the diameter of the cathode is changed. Hence, the distance between the columns is smallest when the largest cathode is utilised and largest when the small cathode is utilised. The five columns are referred to by the letters from A to E. The locations of the five columns are illustrated in figure 7.2.

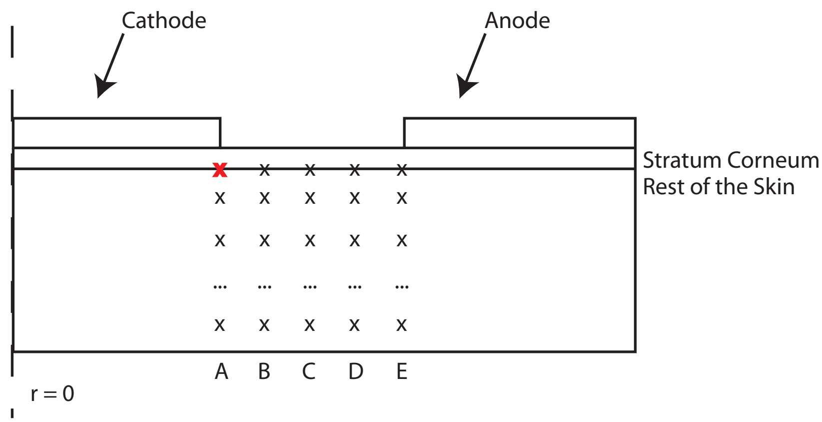

Figure 7.2: shows the sites of the first five columns of probes used to monitor the distribution of the current density in the model of the electric properties of the skin. The columns of probes are referred to by the letters from A to E. All the current densities are normalised according to the current density measured by the probe marked with red

The last five columns are placed in the vicinity of the cathode. The distance between these columns do not change as the previous five, instead the distance is the same regardless of the size of the cathode. The columns are referred to by the roman number from I to V. These probes are used to monitor the change in the vicinity of the cathode, whereas the other probes monitor the current density between the two electrodes. The location of the five columns are illustrated in figure 7.3.

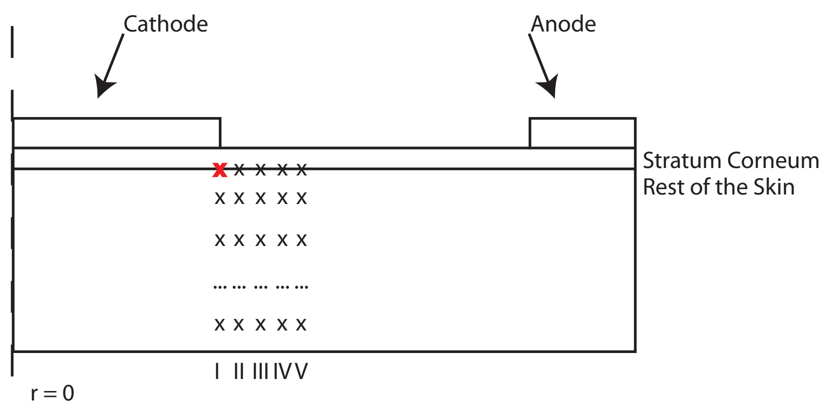

Figure 7.3: shows the sites of the last five columns of probes used to monitor the distribution of the current density in the model of the electric properties of the skin. The columns of probes are referred to by the roman numbers from I to V. All the current densities are normalised according to the current density measured by the probe marked with red

Column A and column I will always be located the same site, at the edge of the cathode. When the largest electrode (d = 20 mm) is utilised the columns A and I, B and II, C and III, D and IV and E and V equal to each other due to the small distance between the anode and the cathode. The probes I to V are monitored in order to increase the resolution near the edge of the cathode.

Ten probes are placed in each of the ten columns at different depths; one in the transition between stratum corneum and the rest skin and the remaining nine are equally distributed in the rest of the skin, as illustrated on figure 7.2 and 7.3. It is chosen not to place an probe in stratum corneum, since it could be observed on figure 7.1 that the current density was very small in this area.

The measured current densities are normalised to the current density measured at the edge of the cathode in the transition between stratum corneum and the remaining skin. Hereby, it is possible to compare the current density at different depths between different electrodes. The measurement conducted by the probe in the first row in the first column will always equal one. This probe is marked with red in figure 7.2 and 7.3. Current densities larger than the current density in this probe will, thereby, be larger than one and vice versa. The rows are referred to by the numbers from 1 to 10.

In the following the results for five different electrode sizes; 0.9 mm, 4 mm, 8 mm, 12 mm and 20 mm, are presented.

Figure 7.4 shows the current density in the different rows, i.e., layers of the skin when the smallest cathode (0.9 mm) is utilised.

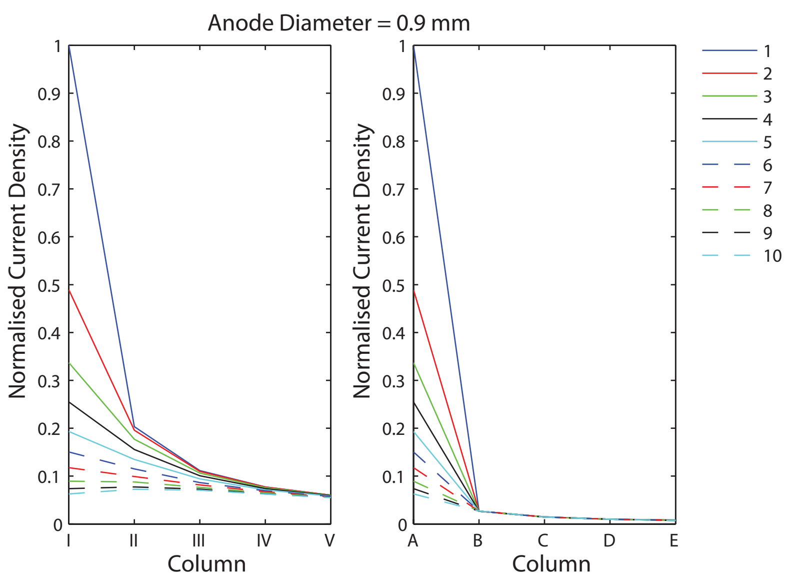

Figure 7.4: shows the current density at different 10 depths in the model of the electric properties of the skin when the cathode with a diameter on 0.9 mm is used. Abscissa refers to the columns, the ordinate is the normalised current density. The figure to the left shows the columns I to V and the figure to the right shows the columns A to E. The columns to the left can be interpreted as an enlargement of the area close to the anode. The legends correspond to the row of the probe

It can be seen from figure 7.4 that the current density is largest in the uppermost layer closest to the cathode. In the second layer, the current density is half of the above. The current density falls further away from the cathode and eventually becomes equally distributed throughout part of the model resembling the skin without stratum corneum. This can also be observed on a surface plot of the distribution of the current density.

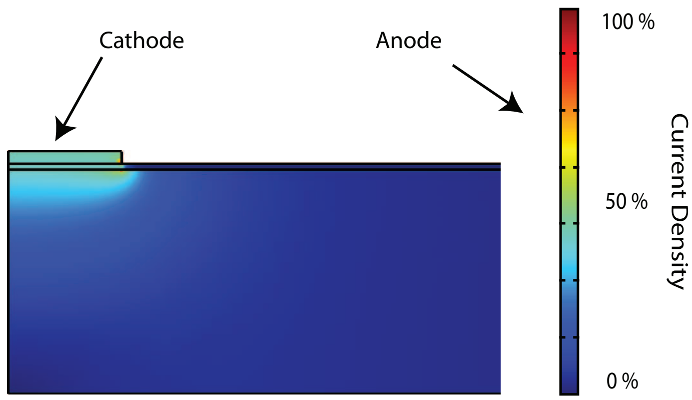

Figure 7.5: shows a surface plot of the current density in the vicinity of the cathode. Only the cathode can be seen, the anode is further to the right

On figure 7.5 it can be seen that the intensity of the current density is largest at the edge of the cathode in the uppermost layers of the skin. In addition, it can be seen that futher towards the anode the current density at different depths of the skin becomes evened out.

The results obtained from the probes when the cathode with a diameter of 4 mm is applied are shown in figure 7.6.

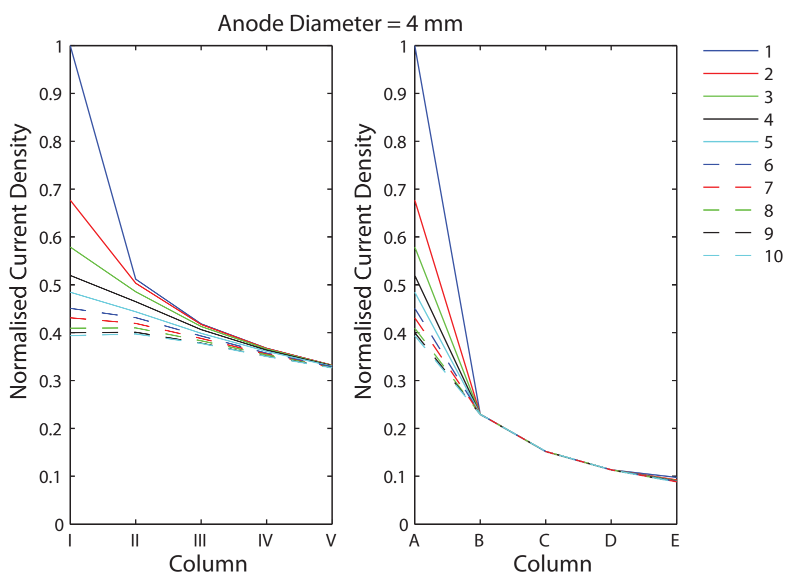

Figure 7.6: shows the current density at different 10 depths in the model of the electric properties of the skin when the cathode with a diameter on 4 mm is used. Abscissa refers to the columns, the ordinate is the normalised current density. The figure to the left shows the columns I to V and the figure to the right shows the columns A to E. The columns to the left can be interpreted as an enlargement of the area close to the cathode. The legends correspond to the row of the probe

The same tendency as when the smaller cathode is utilised can be observed. The decrease is however not as steep.

The measurements conducted when the diameter of the cathode was 8 mm and 12 mm are presented in figure 7.7 and 7.8 respectively.

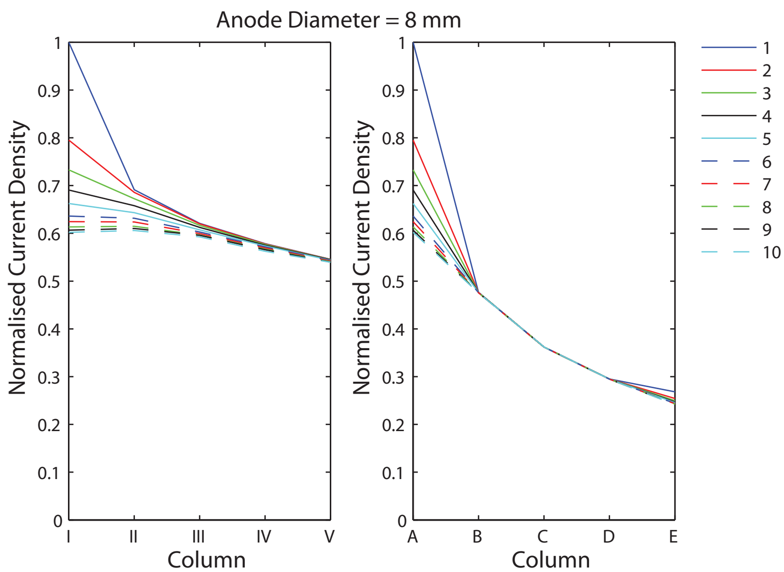

Figure 7.7: shows the current density at different 10 depths in the model of the electric properties of the skin when the cathode with a diameter on 8 mm is used. Abscissa refers to the columns, the ordinate is the normalised current density. The figure to the left shows the columns I to V and the figure to the right shows the columns A to E. The columns to the left can be interpreted as an enlargement of the area close to the cathode. The legends correspond to the row of the probe

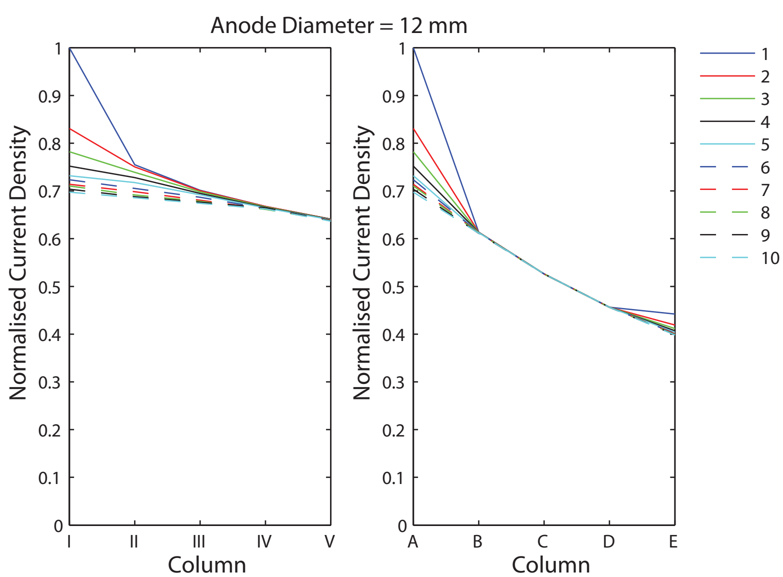

Figure 7.8: shows the current density at different 10 depths in the model of the electric properties of the skin when the cathode with a diameter on 12 mm is used. Abscissa refers to the columns, the ordinate is the normalised current density. The figure to the left shows the columns I to V and the figure to the right shows the columns A to E. The columns to the left can be interpreted as an enlargement of the area close to the cathode. The legends correspond to the row of the probe

The same tendency as with the previous electrodes is observed. However, it can be seen that the current density does not decrease as much as when the smaller cathode are utilised.

In figure 7.9 the normalised current densities measured when the largest cathode, which has a diameter of 20 mm, was applied to the model of the electric properties of the skin.

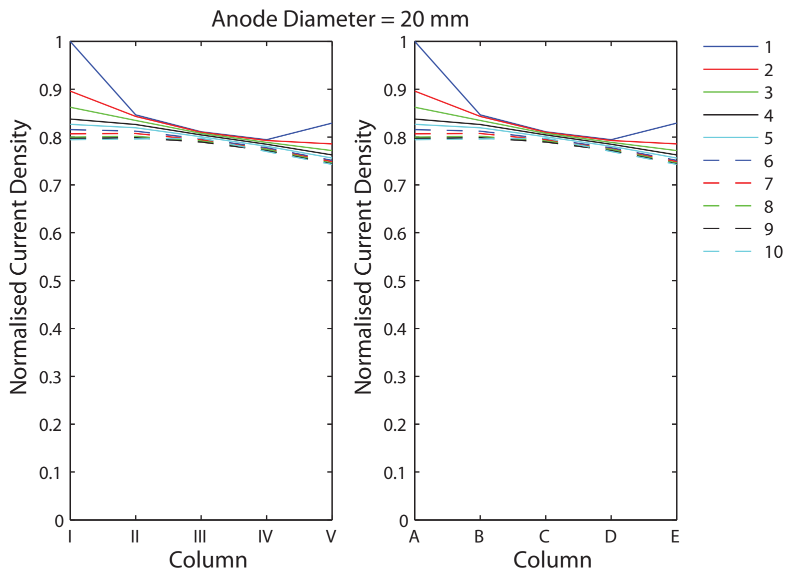

Figure 7.9: shows the current density at different 10 depths in the model of the electric properties of the skin when the cathode with a diameter on 20 mm is used. Abscissa refers to the columns, the ordinate is the normalised current density. The figure to the left shows the columns I to V and the figure to the right shows the columns A to E. The columns to the left can be interpreted as an enlargement of the area close to the cathode. The legends correspond to the row of the probe

In figure 7.10 a surface plot of intensity of the current density is shown. The applied cathode has a diameter of 20 mm. It can, as also seen from the above figure, be seen that the current density does not as rapid as when the smaller electrodes are utilised decrease. However, it is at all layers of the skin kept at a higher intensity.

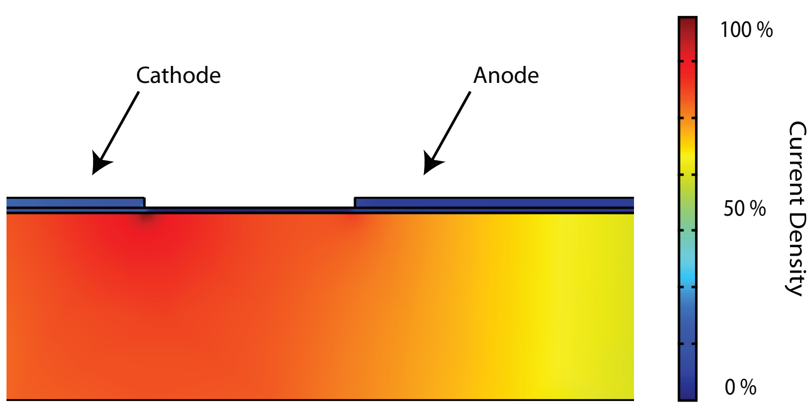

Figure 7.10: shows a surface plot of the current density in the vicinity of the cathode. Only a part of the cathode is shown

It can from figure 7.4, 7.6, 7.7, 7.8 and 7.9 be seen that regardless of the size of the anode the current density becomes equally distributed at some point between the cathode and the anode. The relationship between the current density in the first row in the first column and the current density at the point were it is equally distributed does, however, depend on the size of the cathode. When a small cathode is utilised the current density decreases more than when a larger cathode is utilised.

In order to examine whether the distance between the anode and cathode influences the distribution of the current density the distance between the anode and cathode has been decreased to 1 mm for the cathode with a diameter on 0.9 mm and 12 mm. The current densities measured at in column I to V are shown in figure 7.11 and 7.12 for the cathode with a diameter on 0.9 mm and 12 mm respectively.

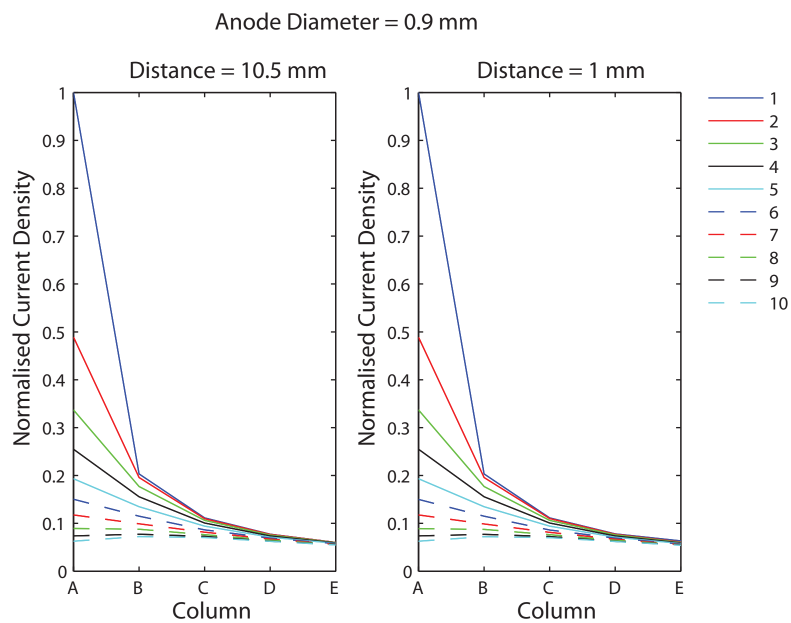

Figure 7.11: shows the normalised current densities obtained from probe in column I to V when the cathode with a diameter on 0.9 mm is utilised. The results shown in figure to the left is when the anode and cathode are 10.5 mm apart, whereas the anode and cathode only are 1 mm apart in the figure to the right. The figure to the left is thereby identical to the left figure in figure 7.4. The legends correspond to the row of the probe

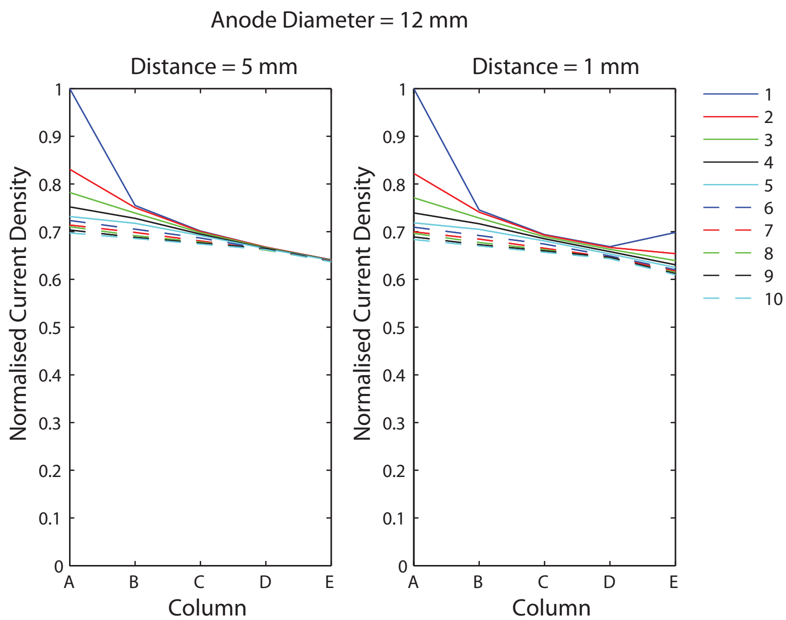

Figure 7.12: shows the normalised current densities obtained from probe in column I to V when the cathode with a diameter on 12 mm is utilised. The results shown in figure to the left is when the anode and cathode are 5 mm apart, whereas the anode and cathode only are 1 mm apart in the figure to the right. The figure to the left is thereby identical to the left figure in figure 7.8. The legends correspond to the row of the probe

It can be seen that the distance of the between the electrode does not alter the relationship between the current density found in the uppermost layer closest to the cathode and the current densities found in the remaining of the skin.

All the above results were obtained when the electric properties of the skin were set to those found at 100 Hz in chapter 4 on page 23. The material properties found at 10, 1000, and 10000 Hz were also tested. However, the relation between the currents densities measured by the probes does not change when another set of material properties is applied. This is shown in figure 7.13, where the current densities obtained when the material properties found at 10, 100, 1000 and 10000 Hz are applied. The shown measurements are for the probes placed in column I to V.

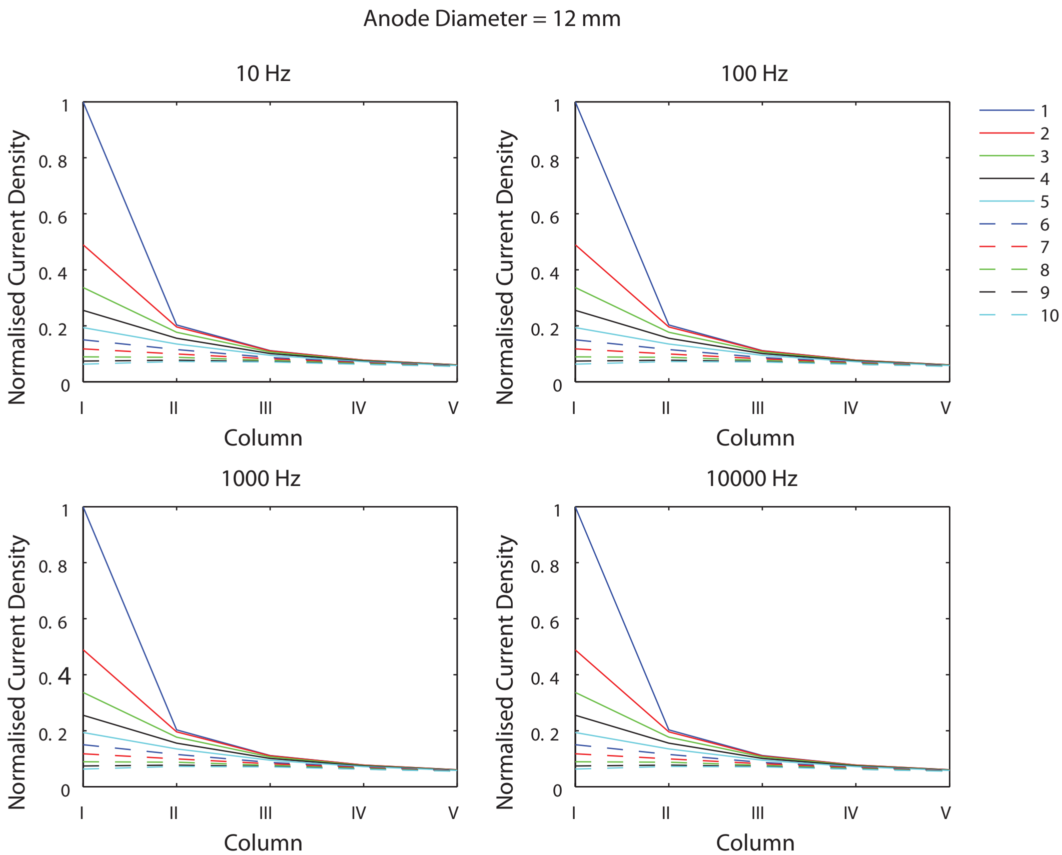

Figure 7.13: shows the normalised current densities obtained from probe in column I to V. The material properties found at 10, 100, 1000 and 10000 Hz are utilised. The legends correspond to the row of the probe

It can be summarised from the above results the distance between the anode and cathode does not influence the current distribution in the skin. Additionally does the results not change when different sets of material properties are applied, i.e., the same results are obtained when the properties found at 10, 100, 1000 and 10000 Hz are applied.

The results indicate that the current densities are evened out in the region between the electrodes. The intensity at which it settle is dependend on the size of the electrode. I.e., the difference between the intensity of the current density in the uppermost layer at the edge of the cathode and the region between the electrodes are larger when a small cathode is utilised, than when a large cathode is utilised. Related to the nerve fibers, it means that when a cathode with the small diameter is used, the nerve fibers located in the upper layers of the skin at the edge of the cathode preferentially will be activated. Whereas when large cathodes are utilised a larger area will contain high current densities and, therefore, nerve fibers in a larger area will be activated, both in the upper and the lower layers of the skin.

Synthesis

IV

Discussion 8

The developed model of the electric properties of the skin is a simplification of the otherwise complex structure of the skin. It is, therefore, important to be aware of the strengths and limitations of the model before evaluating results obtained from the developed model of the electric properties of the skin.

8.1 Methodology

In the developed model the skin only consists of two parts; a thin superficial layer resembling the cornified stratum corneum and a thicker layer resembling the rest of epidermis and the dermis. No further layers were included, e.g., the areolar and adipose tissues of hypodermis. The choice is based on literature findings of the electric properties of the two layers of the skin. The electric properties of the two layers are found by stripping the skin with cellulose-tape. Hence, only the electric properties of stratum corneum and the remaining skin are known. The epidermis is avascular and does only contain limited fluid and the dermis is vascular and contains considerable more fluid than epidermis. Despite this, dermis and the part of epidermis which is not stratum corneum are is treated as one layer in the developed model. This distinction, between the two layers, is, however, of importance when the electric properties are considered. The dermis is presumably a better conductor than epidermis. In order to enhance the model, the layer which now imitates both epidermis and dermis, could be divided. An assumption regarding the distribution of the known conductivity and permittivity could be made. I.e., one third of the conductivity could be assigned to the upper layer and two thirds to the lower layer. This would most likely change the flow of the current. However, it is not certain that it would have changed a result since a comparative study of electrodes with different diameters is conducted.

Besides dividing the skin into further layers, the appendages of the skin could also be taken into consideration. This includes the sweat glands which contain a salt solution. This makes them good conductors. The distribution of sweat glands could, therefore, distort the pathways of the current flow. Sha et al. [2008] developed a finite element model of the skin, which included a sweat gland and found a current density hot spot in the transition between stratum corneum and the rest of the skin adjacent to the sweat gland. The model developed by Sha et al. [2008] did, though, only include the capacitive properties of the stratum corneum. The rest of the skin was considered purely resistive. In the literature survey regarding the electric properties of the skin no studies scrutinizing the skin in such detail were found, thus, the appendages of the skin are explicitly included in the utilised electric properties, even though it is uniformly distributed in the model.

Due to the inhomogeneous structure of the cells the permittivity and conductivity of the skin may not be isotropic. It could be dissembled that the conductivity were lower when approached vertically than when approached horisontally. In order to examine this; an in vitro study must be conducted. However, a comparative study of electrodes with different diameters is conducted and it is not certain that it would have changed the results, even though it might have evened out the differences.

The model of the skin did not extend beyond the cathode, even though, the current probably, if possible, would flow further than the outer edge of the cathode. This constraint is considered acceptable since the current density of interest was in the region between the two electrodes.

The validation of the model showed a lower impedance in the model than in the human skin. Thus, the conductivity of the model might be to low. The conductivity, utilised, was from a study of the electric properties conducted by Yamamoto & Yamamoto [1976*a*], [1976*b*]. The electrodes were left on for 30 minutes to stabilise before the measurement of the permittivity and conductivity was performed. This might have increased the conductivity in the otherwise highly resistive stratum corneum, hence, decreased the impedance. The impedance of the model did, however, show the same tendency as in the impedance measured in the skin. The impedance was higher at low frequencies than at high frequencies.

8.2 Pathways of the Current flow

The results did not show that the current density in general is higher in the more superficial layers than in the lower layers of the skin when a small cathode is utilised. It did, however, indicate that when small electrodes are utilised the current density in the upper layer of the skin, at the edge of the anode is higher compared with the rest of the skin than when anodes with larger diameters are utilised. Thus nerve fibers located in the superficial layers of the skin at the egde of the cathode will preferentially be activated when a small cathode is used. Whereas nerve fibers in a larger area will be affected if larger cathodes are utilised.

In order to scrutinize whether the nociceptors more preferentially are activated, when a cathode with a small diameter is utilised, than when a cathode with a large diameter is utilised, a far more complex model must be developed. Such a model must include the activation threshold of the different nerve fibers found in the skin. In this regard the appendages of the skin will be of greater importance, since they might cause areas with increased current densities, as seen in the study conducted by Sha et al. [2008], and, thereby, increase the activation of the nerve fibers.

9 Conclusion

This project focused on how nociceptors more preferentially than other cutaneous sensory organs and nerve fibers could be activated due to an applied electric current. A literature study revealed different designs of surface electrodes utilised to activate the nociceptors without activating the other cutaneous sensory organs and nerve fibers.

To determine whether the different electrodes preferentially activated the nociceptor conduction velocities of the nerve fibers and subjective parameters as flare and pain intensity were measured. However, it was not known whether the other sensory organs and nerve fibers also were activated. In order to preferentially stimulate the nociceptors, it is adequate that the current intensity in the uppermost layers of the skin is much higher than in the remaining skin, due to location of the nociceptors. Based on this and on literature findings the following thesis statement was expressed:

A concentric surface electrode with a small diameter will cause the applied current to flow in the more superficial layers of the skin, than a concentric surface electrode with a larger diameter.

A concentric electrode with a cathode in the center and a surrounding anode was utilised. The diameter of the cathode could be changed between the following sizes; 0.9, 4, 8, 12 and 20 mm.

In order to test the thesis a finite element model was developed taking the thickness and the electric properties of the layers of the skin into account. The utilised thicknesses and the electric properties of the skin were based on litterature findings. The finite element model was developed in COMSOL Multiphysics 3.5. The model was validated by comparing impedance of human skin with the impedance of the model. The model showed a smaller impedance than the measurements obtianed from the experiment, but showed the same tendency due to change in frequency.

From the results obtained from the model, it could be concluded that the current density not in general was higher in the more superficial layers than lower layers of the skin. It could, though, be concluded that the current density in the upper layers of the skin at the edge of the cathode was much higher than in the rest of the skin. This finding was independent of the distance between the anode and the cathode and independent of which frequency was utilised. A small electrode will, therefore, more preferentially stimulate nociceptors than a large electrode.

Bibliography

Andersen, O. K. [2007], 'Studies of the organization of the human nociceptive withdrawal reflex. focus on sensory convergence and stimulation site dependency', Acta Physiologica, Center for Sensory-Motor Interaction.

Anne [2003], Internet. http://www.ratbehavior.org/images/Epidermis.jpg.

Dewarrat, F., Falco, L., Talary, M. S., Feldman, Y. & Puzenko, A. [2008], 'Measurement and simulation of conductive dielectric two-layer materials with a multiple electrodes sensor', *IEEE Transactions on Dielectrics and Electrical Insulation* .

Djouhri, L. & Lawson, S. [2004], 'Abeta-fiber nociceptive primary afferent neurons: a review of incidence and properties in relation to other afferent a-fiber neurons in mammals', *Brain Research Reviews* **46**.

Ebert, H. & Raskmark, P. [1998], Grundlæggende maxwellsk feltteori. Aalborg Universitet.

Foster, K. R. & Lukaski, H. C. [1996], 'Whole-body impedance - what does it measure?', *American Society for clinical Nutrition* **64**.

Gabriel, C. [1997], 'Comments on t'dielectric properties of the skint'', *Phys. Med. Biol.* **42**.

Gabriel, C., Gabriel, S. & Corthout, E. [1996], 'The dielectric properties of biological tissues: I. literature survey', *Phys. Med. Biol.* **41**.

Gabriel, S., Lau, R. W. & Gabriel, C. [1996*a*], 'The dielectric properties of biological tissues: Ii. measurements in the frequency range 10 hz to 20 ghz', *Phys. Med. Biol.* **41**.

Gabriel, S., Lau, R. W. & Gabriel, C. [1996*b*], 'The dielectric properties of biological tissues: Ii. parametric models for the dielectric spectrum of tissues', *Phys. Med. Biol.* **41**.

Grimnes, S. & Øjran G. Martinsen [2000], *Bioimpedance and Bioelectricity*, Academic Press.

Inui, K., Tran, T. D., Hashoyama, M. & Kakigi, R. [2001], 'Preferential stimulation of aδ fibers by intra-epidermal needle electrode in humans', *Pain* **96**.

Jung, K., Rottmann, S. & Ellrich, J. [2009], 'Long-term depression of spinal nociception and pain in man: Influence of varying stimulation parameters', *European Journal of Pain* **13**.

Kahle, W. & Frotscher, M. [2003], *Color Atlas of Human Anatomy Nervous System and Sensory Organs*, Vol. 3, 5 edn, Elsevier.

Kandel, E. R., Schwartz, J. H. & Jessell, T. M. [1991], *Principles of Neural Science*, 4 edn, McGraw-Hill, chapter 36. Spinal Reflexes, pp. 713–736.

Katsarava, Z., Ayzenberg, I., Sack, F., Limmroth, V., Diener, H.-C. & Kaube, H. [2006], 'A novel method of eleciting pain-related potentials by transcutaneous electric stimulation', *Headache* **46**.

Klein, T., Magerl, W., Hopf, H. C., Sandkuhler, J. & Treede, R. D. [2004], 'Perceptual correlates of nociceptive long-term potentiation and long-term depression in humans.', *Journal of Neuroscience* **24**.

Lahtinen, T., Nuutien, J. & Alanen, E. [1997], 'Dielectric properties of the skin', *Phys. Med. Biol.* **42**.

Lawson, R. [n.d.], Internet. http://upload.wikimedia.org/wikibooks/en/2/23/.

Martini, F. H. [2004], *Fundamentals of Human Anatomy & Physiology*, 6 edn, Pearson Education Int.

McMahon, S. & Kolzenburg, M. [2006], *Wall and Melzack's Textbook of Pain*, 5 edn, Elsevier.

Moore, T. L., Lunt, M., McManus, B., Anderson, M. E. & Herrick, A. L. [2003], 'Seventeen-point dermal ultrasound scoring system - a reliable measure of skin thickness in patients with systemic sclerosis', *Rheumatology* **42**.

Multiphysics, C. [2008], *AC/DC Module - User's Guide*, Comsolab.

Neerken, S., Lucassen, G. W., Bisschop, M. A., Lenderink, E. & Nuijs, T. A. [2004], 'Characterization of age-related effects in human skin: A comparative study that applies confocal laser scanning microscopy and optical coherence tomography', *Journal of Biomedical Optics* **9**.

Nilsson, H.-J., Levinsson, A. & Schouenborg, J. [1996], 'Cutaneous field stimulation (cfs): a new powerfil method to combat itch', *Pain* **71**.

Reilly, J. P. [1998], *Applied Bioelectricity - From Electrical Stimulation to Electropathology*, Springer.

Ørjan G. Martinsen, Grimnes, S. & Schwan, H. P. [2002], 'Interface phenomena and dielectric properties of biological tissue', *Encyclopedia of Surface and Colloid Science* .

Sandby-Møller, J., Poulsen, T. & Wulf, C. [2003], 'Epidermal thickness at different body sitess: Relationship to age, gender, pigmentation, blood content, skin type and smoking habits.', *Acta Derm Venereol* **83**.

Schibye, B. & Klausen, K. [2004], *Menneskets Fysiologi - Hvile og arbejde*, Vol. 1, 9 edn, FADL.

Serway, R. A. & Jewett, J. W. [2004], *Physics for Scientists and Engineers with Modern Physics*, 6 edn, Thomson.

Sha, N., Kenney, L. P., Heller, B. W., Barker, A. T., Howard, D. & Moatamedi, M. [2008], 'A finite element model to identify electrode influence on current distribution in the skin', *Artificial Organs* **32**.

Standring, S. [2005], *Gray's Anatomy*, 39 edn, Elsevier.

Volakis, J. L., Chatterjee, A. & Kempel, L. C. [1998], *Finite Element Method for Electromagnetics*, IEEE press.

Yamamoto, T. & Yamamoto, Y. [1976*a*], 'Dielectric constant and resistivity of epidermal stratum corneum', *Medical and Biological Engineering* .

Yamamoto, T. & Yamamoto, Y. [1976*b*], 'Electrical properties of the epidermal stratum corneum', *Medical and Biological Engineering* .

Yoshida, K., Inmann, A. & Haugland, M. K. [1999], 'Measurement of complex impedance spectra of implanted electrodes'. http://www.ifess.org/ifess99/Poster%20Session/yoshida.htm.

Yosipovitch, G., Carstens, E. & McGlone, F. [2007], 'Cronic itch and chronic pain: Analogous mechanisms', *Pain* **131**.

Verification of the model

A

The calculations made in the finite element model developed in COMSOL multiphysics 3.5 must be verified to be able to rely on the developed model. In addition it will become obvious if the wrong application is utilised. The model of the electric properties of the skin is developed in axial symmetry in 2D with in the AC/DC module with the quasi-static, electric approximation. The verification was conducted by developing a simpler model resembling the original model. The new model consists of two layers with a electrode in the top and in the bottom. In the new model it is more straight forward to manually calculate the resulting current, than in the model developed to test the hypothesis. An electric analogy of the new model can easily be found and the resulting current calculated. This current is, hereafter, compared to the current obtained in the model from COMSOL. The current is uniform throughout each model and can therefore easily be used to validate the model.

The electric analogies can be made as long as the physical extent, d is [Ebert & Raskmark 1998]:

$$d << \frac{\lambda}{2\pi} \tag{A.1}$$

where λ is the wavelength of the applied signal. The wavelenght depends on the electric properties of the material it propagates in. The wavelenghts in the skin at different frequencies have been calculated in chapther **??**. The smallest wavelenght was 10 meter, this means that the extent of the model used to verify the calculations must be much smaller than 10 meter/$2\pi \approx 1.5$ meters, if electric analogies are utilised to verify the model.

The model developed to verify the calculations made is shown in figure A.1. Each of the to layers are 0.04 meters high and have a diameter on 0.08 meter.

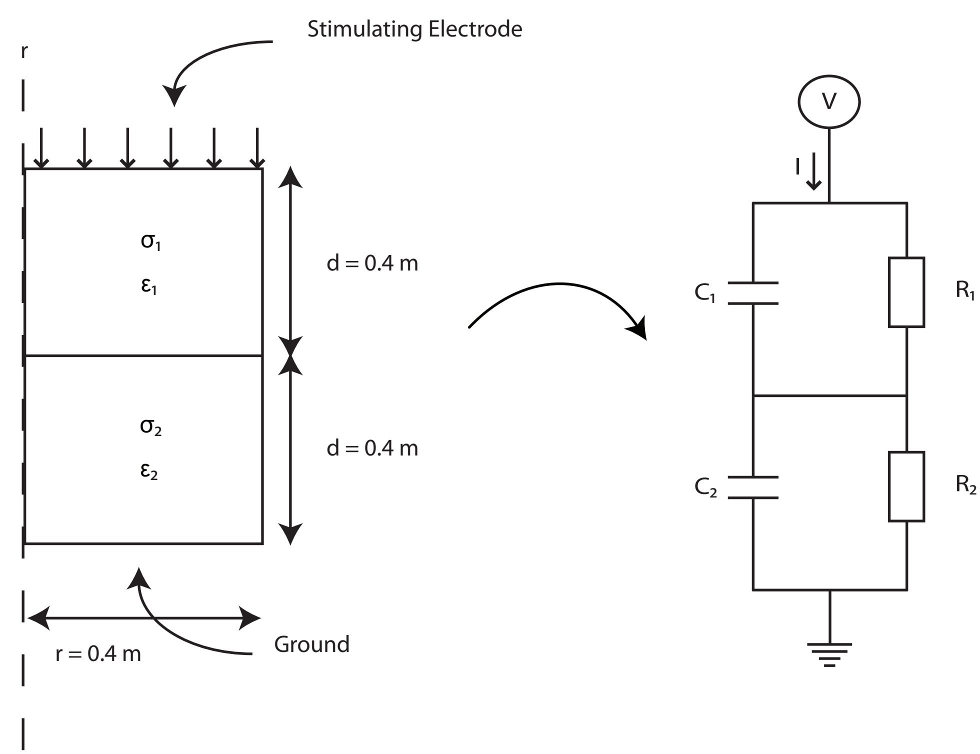

Figure A.1: illustrates the second model developed to verify the calculations made by COMSOL.

To the left in the figure the model created in COMSOL is shown and to the right the electric analogy of the model is shown. The current through the electric analogy can be calculated by Laplace transforming and applying Ohms law, thereby, the following equation:

$$I = V / \left(\frac{R_1}{s \cdot C_1 \cdot R_1 + 1} + \frac{R_2}{s \cdot C_2 \cdot R_2 + 1} \right) \tag{A.2}$$

where $s = j\omega$. As described in section **??** on page **??** the resistor is defined by its conductive properties, σ, whereas the capacitor is defined by its permittivity, ε:

$$R = \frac{d}{\sigma A} \tag{A.3}$$

$$C = \frac{\varepsilon_0 \varepsilon_r \cdot A}{d} \tag{A.4}$$

where d is the distance and A is the area defined in the model to the left in figure A.1. Since the model is developed with axial symmetry the area becomes: $A = \pi r^2$.

This model is verified by appling the electric properies of the stratum corneum and the rest of the skin found at the frequencies; 10, 100, 1000 and 10.000 Hz in chapter 4.

The resulting currents were compared visually and found to be in agreement. COMSOL is, therefore, believed to calculate correctly when a model consisting of several layers developed. In figure A.2 a part of the found current is plotted. The shown currents are obtained when the the electric properties of the skin found at 10.000 Hz are utilised.

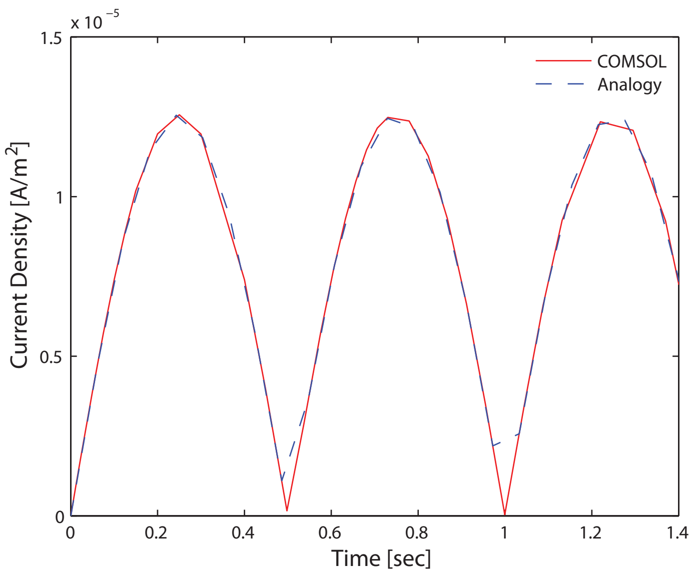

Figure A.2: shows the current in the model developed to verify the model and the electric analogy of the skin. The parameters used corresponds to those found for the skin at 10.000 Hz